

Papers in Honour of Ken Aplin

edited by

Julien Louys, Sue O'Connor and Kristofer M. Helgen

Helgen, Kristofer M., Julien Louys, and Sue O'Connor. 2020. The lives of creatures obscure, misunderstood, and wonderful: a volume in honour of Ken Aplin 1958–2019	149
Armstrong, Kyle N., Ken Aplin, and Masaharu Motokawa. 2020. A new species of extinct False Vampire Bat (<i>Megadermatidae: Macroderma</i>) from the Kimberley Region of Western Australia	161
Cramb, Jonathan, Scott A. Hocknull, and Gilbert J. Price. 2020. Fossil <i>Uromys</i> (Rodentia: Murinae) from central Queensland, with a description of a new Middle Pleistocene species	175
Price, Gilbert J., Jonathan Cramb, Julien Louys, Kenny J. Travouillon, Eleanor M. A. Pease, Yue-xing Feng, Jian-xin Zhao, and Douglas Irvin. 2020. Late Quaternary fossil vertebrates of the Broken River karst area, northern Queensland, Australia	193
Theden-Ringl, Fenja, Geoffrey S. Hope, Kathleen P. Hislop, and Benedict J. Keaney. 2020. Characterizing environmental change and species' histories from stratified faunal records in southeastern Australia: a regional review and a case study for the early to middle Holocene	207
Brockwell, Sally, and Ken Aplin. 2020. Fauna on the floodplains: late Holocene culture and landscape on the sub-coastal plains of northern Australia	225
Hawkins, Stuart, Fayeza Shasliz Arumdhathi, Mirani Litster, Tse Siang Lim, Gina Basile, Mathieu Leclerc, Christian Reepmeyer, Tim Ryan Maloney, Clara Boulanger, Julien Louys, Mahirta, Geoff Clark, Gendro Keling, Richard C. Willan, Pratiwi Yuwono, and Sue O'Connor. 2020. Metal-Age maritime culture at Jareng Bori rockshelter, Pantar Island, eastern Indonesia	237
Frankham, Greta J., Linda E. Neaves, and Mark D. B. Eldridge. 2020. Genetic relationships of Long-nosed Potoroos <i>Potorous tridactylus</i> (Kerr, 1792) from the Bass Strait Islands, with notes on the subspecies <i>Potorous tridactylus benormi</i> Courtney, 1963	263
Rowe, Kevin C., Helena A. Soini, Karen M. C. Rowe, Mark Adams, and Milos V. Novotny. 2020. Odorants differentiate Australian <i>Rattus</i> with increased complexity in sympatry	271
Louys, Julien, Michael B. Herrera, Vicki A. Thomson, Andrew S. Wiewel, Stephen C. Donnellan, Sue O'Connor, and Ken Aplin. 2020. Expanding population edge craniometrics and genetics provide insights into dispersal of commensal rats through Nusa Tenggara, Indonesia	287
Breed, William G., Chris M. Leigh, and Eleanor J. Peirce. 2020. Reproductive biology of the mice and rats (family Muridae) in New Guinea—diversity and evolution	303
Suzuki, Hitoshi. 2020. Evolutionary history of the subgenus <i>Mus</i> in Eurasia with special emphasis on the House Mouse <i>Mus musculus</i>	317
Richards, Stephen J., and Stephen C. Donnellan. 2020. <i>Litoria aplini</i> sp. nov., a new species of treefrog (Pelodyadidae) from Papua New Guinea	325

Records of the Australian Museum

volume 72, issue no. 5

25 November 2020



Fossil *Uromys* (Rodentia: Murinae) from Central Queensland, with a Description of a New Middle Pleistocene Species

JONATHAN CRAMB^{1,2} , SCOTT A. HOCKNULL^{1,3} , AND GILBERT J. PRICE² 

¹ Geosciences, Queensland Museum, 122 Gerler Road, Hendra QLD 4011, Australia

² School of Earth and Environmental Sciences, The University of Queensland, Brisbane QLD 4072, Australia

³ School of BioSciences, Faculty of Science, University of Melbourne, Melbourne VIC 3010, Australia

ABSTRACT. The first fossil species of *Uromys* (Giant Naked-tailed Rats) is described, as well as the southern-most records of the genus based on palaeontological data. *Uromys aplini* sp. nov. lived during the Middle Pleistocene in the area around Mount Etna, eastern central Queensland, but was probably driven extinct by climate-mediated habitat loss sometime after 205 ka but before c. 90 ka. A second species, the extant *U. caudimaculatus*, occurred in the area during the Late Pleistocene, but became locally extinct prior to the Last Glacial Maximum. These fossils indicate an unexpectedly high diversity of species of *Uromys* in Australia, suggesting a long occupation of the continent. Phylogenetic analysis places *U. aplini* together with other species of *Uromys* endemic to Australia, at the base of the radiation of the genus. This may indicate that the initial diversification of *Uromys* occurred in Australia rather than New Guinea, as has previously been thought. These new Quaternary records of *Uromys* occur approximately 550 km south of the southern-most modern record for the genus, indicating that *Uromys* was able to cross the southern St Lawrence biogeographic barrier, possibly twice during the Pleistocene.

Introduction

Uromys (commonly called “Giant Rats” or “Giant Naked-tailed Rats”) is a genus of generally very large murine rodents whose species are found on mainland and continental islands of northern Sahul (Australia and New Guinea), and the Melanesian island archipelago (Fig. 1). They belong to the tribe Hydromyini, in a subclade called the *Uromys* division (colloquially known as the “Mosaic-tailed Rats”), that also includes four related genera: *Melomys*, *Paramelomys*, *Protochromys*, and *Solomys* (Musser & Carleton, 2005; Lecompte *et al.*, 2008; Aplin & Helgen, 2010). The ecology and conservation status of extant species of *Uromys* was summarized by Flannery (1995a, 1995b), Breed & Ford (2007), Moore (2008), and Moore & Winter (2008). These authors noted that many species are presently endangered, critically endangered or presumed extinct.

Currently, 11 species of *Uromys* are recognized. Two widely distributed and morphologically variable species occur on mainland New Guinea (*U. anak* and *U. caudimaculatus*, the latter also occurring on several nearby islands), with a further four near threatened to critically endangered species that are endemic to the nearby islands of Biak (*U. boeadii*), Awai (*U. emmae*), New Britain (*U. neobritannicus*) and Kai Besar (*U. siebersi*) (Flannery, 1995a, 1995b; Musser & Carleton, 2005). Four species are recorded from the Solomon Islands, namely *U. imperator*, *U. porculus*, *U. rex*, and *U. vika*, all of which are either endangered, critically endangered or presumed recently extinct (Flannery, 1995b; Lavery & Judge, 2017; taxonomic authorities listed below).

In Australia, two species of *Uromys* are currently recognized (Breed & Ford, 2007). *Uromys caudimaculatus* has a distribution stretching from Cape York to the most

Keywords: Hydromyini; Muridae; rainforest; extinction

Taxonomic registration: urn:lsid:zoobank.org:pub:BEE60C62-CA61-48C2-B8EB-E7DAC94FEA09

Corresponding author: Jonathan Cramb j2.cramb@connect.qut.edu.au

Received: 3 February 2020 **Accepted:** 20 August 2020 **Published:** 25 November 2020 (in print and online simultaneously)

Publisher: The Australian Museum, Sydney, Australia (a statutory authority of, and principally funded by, the NSW State Government)

Citation: Cramb, Jonathan, Scott A. Hocknull, and Gilbert J. Price. 2020. Fossil *Uromys* (Rodentia: Murinae) from central Queensland, with a description of a new Middle Pleistocene species. In *Papers in Honour of Ken Aplin*, ed. Julien Louys, Sue O'Connor, and Kristofer M. Helgen. *Records of the Australian Museum* 72(5): 175–191. <https://doi.org/10.3853/j.2201-4349.72.2020.1731>

Copyright: © 2020 Cramb, Hocknull, Price. This is an open access article licensed under a Creative Commons Attribution 4.0 International License (CC BY 4.0), which permits unrestricted use, distribution, and reproduction in any medium, provided the original authors and source are credited.



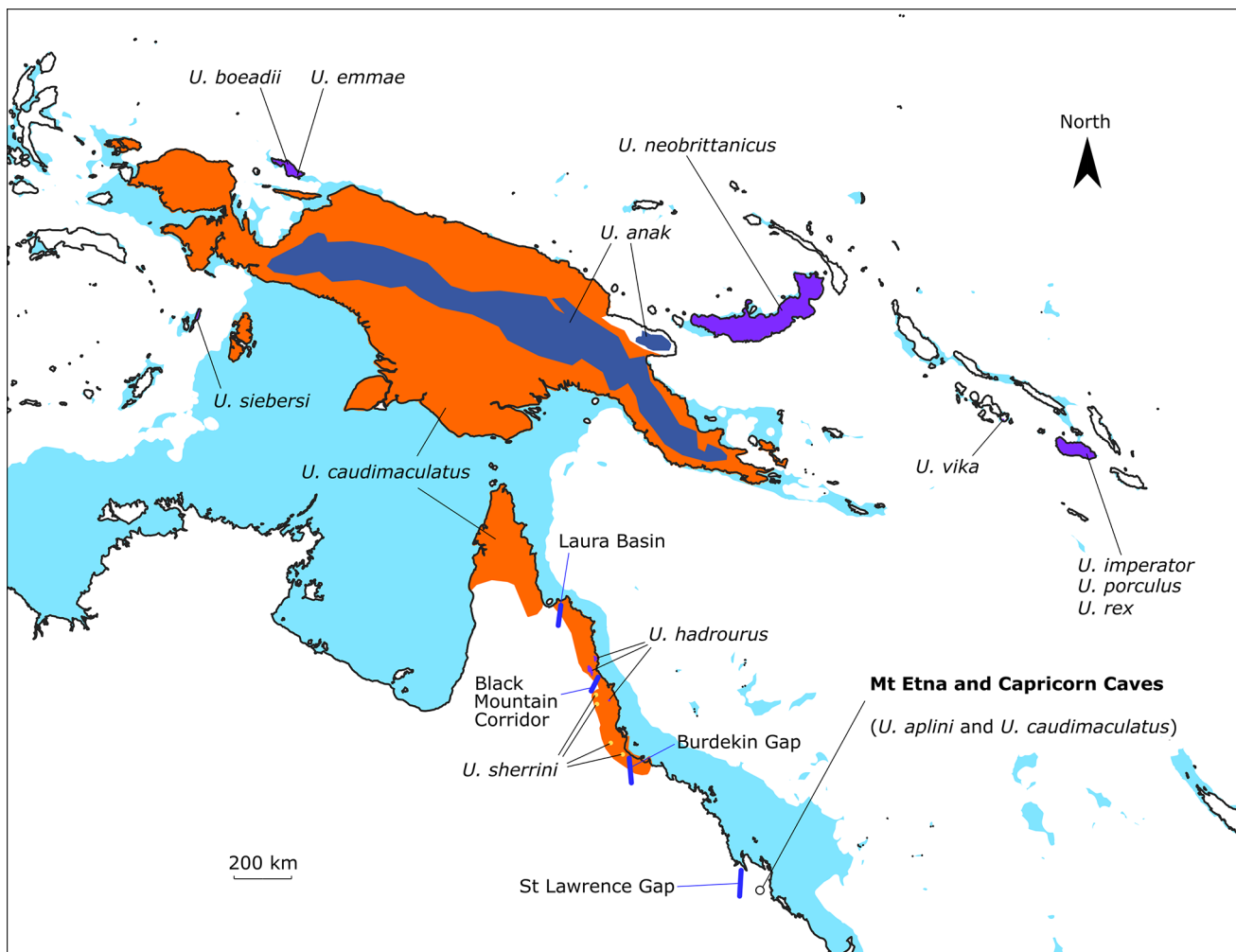


Figure 1. Map of north-east Sahul and Melanesia showing the location of study sites, the modern distributions of species of *Uromys*, and barriers to dispersal of mesic taxa in eastern Queensland (after Bryant & Krosch, 2016). Bathymetric depth to 200 m marked in light blue. Distribution data is from Aplin & Flannery (2017), Aplin *et al.* (2017), Groves & Flannery (1994), Kennerley (2016), Lavery (2019), and Woinarski & Burbidge (2016). Spot distribution of *U. sherrini* is based on known specimens in the collections of the Queensland Museum, CSIRO National Wildlife Collection, and Natural History Museum (London).

southerly modern occurrence of the genus, just south of Townsville in the Bowling Green National Park (Moore, 2008); QMJM1248 from Atlas of Living Australia website at <https://www.ala.org.au/> (accessed 10 January 2020). The taxonomic history of Australian populations of *U. caudimaculatus*, and extralimital taxa synonymized with it, was summarized by Jackson & Groves (2015). The second, smaller Australian species, *U. hadrourus*, is restricted to the upland regions of north-east Queensland (Atherton Tableland, Mount Carbine, Thornton Peak, and Mount Bartle Frere). A third taxon, *U. sherrini*, described originally by Thomas (1923a), is currently considered to be a junior synonym of *U. caudimaculatus* (Tate, 1951), but Kristofer Helgen and Ken Aplin (pers. comm. November 2009) considered *U. sherrini* to be distinct from *U. caudimaculatus* on the basis of unpublished morphological and molecular comparisons. We therefore treat it as a separate species in this study.

The evolutionary history of Australian rodents has been investigated in recent decades using several lines of morphological (e.g., craniodental, phallic, and spermatozoan morphology) and molecular evidence to assess phylogeny

(e.g., Lidicker & Brylski, 1987; Groves & Flannery, 1994; Breed & Aplin, 1995; Rowe *et al.*, 2008; Robins *et al.*, 2010; Stepan & Schenk, 2017). Molecular sampling of hydromyine taxa is incomplete, and meta-analyses that include broad taxonomic sampling have recovered specific or generic level relationships that are questionable. For example, Upham *et al.* (2019), in their meta-analysis of mammalian phylogenies recovered *Pithecheir* as the sister taxon of *Uromys*, despite the placement of these genera in different divisions by other authors (Musser & Carleton, 2005). Bryant *et al.* (2011) and Lavery & Judge (2017) both conducted molecular analyses of *Uromys* division taxa, but unfortunately did not include the majority of species of *Uromys*. Bryant *et al.* (2011) did, however, recover *Paramelomys* as the sister taxon to a clade containing *Melomys*, *Solomys*, and *Uromys*, providing a potentially useful outgroup for any morphological assessment of phylogeny. Morphological phylogenetic methods are obviously of vital importance to palaeontological studies, but we are aware of only one published example that included Australian species of *Uromys*: Groves & Flannery (1994) in their revision of the genus.

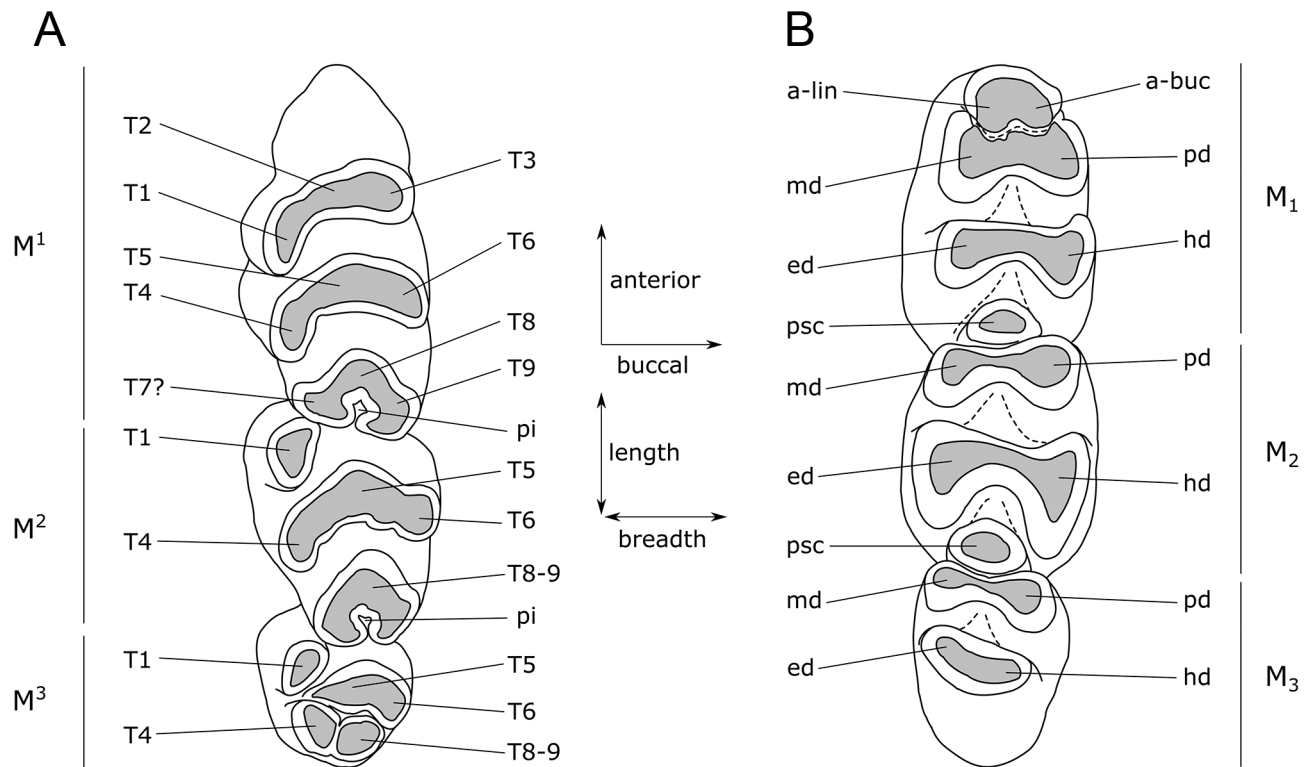


Figure 2. Molar cusp terminology. In *Uromys* and closely related genera the cusps in each molar loph are fused, so individual cusps may be difficult to distinguish in worn specimens. Molar terminology follows Musser (1981), Aplin & Helgen (2010), and Lazzari *et al.* (2010). (A) upper molars, left side in occlusal outline; (B) lower molars, right side, in occlusal outline. Abbreviations: *a-buc*, antero-buccal cuspid; *a-lin*, antero-lingual cuspid; *ed*, entoconid; *hd*, hypoconid; *md*, metaconid; *pd*, protoconid; *pi*, posterior indent; *psc*, posteroconid.

With the majority of species of *Uromys* found in New Guinea and Melanesia, it has long been assumed that *Uromys* had its phylogenetic origin in these regions; Watts & Aslin (1981) posited that *Uromys* was a relatively recent arrival in Australia, having crossed the Torres Strait during the Last Glacial Maximum. This view was not held by all researchers with Tate (1951) suggesting that *Uromys* arrived in Australia during the Middle Pleistocene, and Hand (1984) stating that the timing of arrival was unclear. The recognition that *U. hadrourus* was a species of *Uromys* rather than a species of *Melomys* (see Jackson & Groves, 2015) hinted that *Uromys* had been present in Australia for some substantial time, with Aplin (2006) citing Watts and Baverstock's (1994) molecular data to suggest the possibility that the genus was present before 2.5 Ma. Such a possibility would be supported if fossils of the right age were available. Despite the presence of murines in Sahul since at least 4.18 Ma (Piper *et al.*, 2006), published reports of fossil *Uromys* are almost all restricted to the Late Pleistocene and Holocene (e.g., O'Connor *et al.*, 2002; Aplin *et al.*, 1999). The exception is Hocknull (2005), who reported a large Mosaic-tailed Rat from the Mount Etna caves, which was later found to be of Middle Pleistocene age (Hocknull *et al.*, 2007). This taxon is here described as *Uromys aplini* sp. nov., and is the geologically oldest species of the genus yet recorded.

Materials and methods

All fossil specimens included in this study were excavated as part of ongoing research into the fossils of the caves in the Mount Etna and Capricorn Caves region, eastern central Queensland (Fig. 1). Fossils were compared with specimens of all available species of *Uromys* in the collections of the Queensland Museum, Australian Museum, and the Australian National Wildlife Collection (Appendix 1). Where specimens of some species were not available in Australian collections, comparisons with published descriptions and images were made. Fossil specimens were measured with digital callipers, and imaged with a Visionary Digital "passport storm" camera system, an Olympus Stylus TG-4 compact digital camera, a Hitachi TM-1000 environmental scanning electron microscope at the Queensland Museum, and a Leica DFC450 C digital microscope camera at the School of Earth and Environmental Sciences, The University of Queensland. All fossils described in this paper are catalogued in the collections of the Queensland Museum, in Brisbane, Australia. Molar cusp terminology is presented in Fig. 2.

Study sites background

Fossil remains described here were collected from cavernous limestone located at the Mount Etna and Limestone Ridge Caves National Park and the Capricorn Caves Tourist Park (Hocknull, 2005, 2009; Price *et al.*, 2015). The bulk of fossils

Table 1. Character matrix used in phylogenetic analysis. Modified from Groves & Flannery (1994). Note that the original numbering of characters is retained from Groves & Flannery (1994), although external characters are removed. Additional characters: (50) M^{1-3} length: 0 = 7 mm, 1 = 7–8 mm, 2 = 8–9 mm, 3 = 9–10 mm, 4 = 10–11 mm, 5 = 11–12 mm, 6 = 12–13 mm, 7 = 13–14 mm; (51) M^{1-3} length/ M^1 width: 0 = 3–3.2, 1 = 3.2–3.4, 2 = 3.4–3.6, 3 = 3.6–3.8, 4 = 3.8–4.0.

	1	2	3	4	5	6	7	8	9	0	1	1	1	1	1	1	1	1	2	2	2	2	2	2	2	3	3	3	4	4	4	4	4	4	4	4	5	5		
<i>Paramelomys rubex</i>	1	?	?	?	0	0	0	?	?	1	1	0	0	0	0	1	?	0	1	?	0	?	0	0	0	0	0	1	1	0	1	1	1	0	0	1	0	0	0	1
<i>Uromys anak</i>	0	1	0	1	1	1	1	0	1	0	1	0	1	0	0	0	1	0	1	1	0	1	0	0	0	0	0	0	1	1	1	0	1	0	0	0	0	{6,7}	{1,2,3}	
<i>U. aplini</i> sp. nov.	1	?	?	?	1	0	0	?	?	1	1	0	1	0	0	?	?	1	?	?	0	?	?	0	0	0	1	?	?	1	1	1	0	1	?	?	?	0	{3,4}	2
<i>U. boeadii</i>	0	1	0	1	0	0	0	0	0	0	0	0	0	0	0	0	0	0	1	0	0	1	0	0	0	0	0	0	1	1	1	0	1	0	0	0	5	2		
<i>U. caudimaculatus</i>	1	1	1	1	1	0	1	0	1	1	0	0	1	0	0	1	1	1	1	0	0	0	0	0	0	0	1	1	1	1	1	0	1	1	0	0	{5,6}	{1,2,3,4}		
<i>U. emmae</i>	1	1	1	1	1	0	1	0	1	1	0	0	1	0	0	1	0	0	1	0	0	0	0	0	0	0	1	0	1	1	1	0	1	1	0	1	5	2		
<i>U. hadrourus</i>	1	1	1	1	1	0	0	0	1	1	1	0	1	0	1	1	0	1	1	0	0	0	0	0	0	1	1	1	1	1	0	1	1	1	0	{1,2}	{0,1,2,3}			
<i>U. imperator</i>	1	0	1	0	0	1	0	1	0	1	0	0	1	1	0	0	0	0	0	1	0	1	0	0	1	1	0	0	1	0	0	0	1	0	0	0	6	1		
<i>U. neobritannicus</i>	0	1	0	1	1	0	1	0	1	0	1	0	1	0	0	0	0	0	1	1	0	1	0	0	0	0	0	0	1	1	1	0	1	0	0	{6,7}	{2,3}			
<i>U. porculus</i>	0	0	0	0	0	1	0	1	0	0	0	0	1	1	0	0	0	0	0	1	0	1	0	0	1	1	0	0	1	0	0	0	0	0	0	0	0	2		
<i>U. rex</i>	0	0	1	0	0	1	0	1	0	1	1	1	1	1	0	0	0	0	0	1	1	1	1	1	1	0	0	1	0	0	0	0	0	0	0	{4,5}	{1,2}			
<i>U. sherrini</i>	1	?	?	?	1	0	0	?	?	1	1	0	1	0	0	0	?	0	1	?	0	?	0	0	0	0	1	1	1	1	1	0	1	1	0	{5,6}	{1,2}			
<i>U. vika</i>	0	?	?	?	0	1	0	?	?	1	1	?	1	0	0	0	?	0	1	?	0	?	1	0	0	1	?	1	0	1	0	1	0	?	0	0	0	2	1	

from the deposits are most likely derived from the feeding activities of owls. Fossil deposits from Mount Etna were described initially by Hocknull (2005) with biocorrelation of these faunas suggesting a Pliocene age. Subsequent radiometric dating of flowstones associated with the fauna demonstrated, however, that these deposits were in fact Pleistocene in age and restricted to the Middle Pleistocene (Hocknull *et al.*, 2007). Additional sites, descriptions, and dating assessments were also undertaken and available in Hocknull (2009). At Capricorn Caves Tourist Park, Queensland Museum Locality (QML) 1456 is located within the Olsen’s Cave system. Faunal remains recovered from this site were described and chronometrically dated using a combination of radiocarbon and uranium-series techniques, resulting in a Late Pleistocene age (Price *et al.*, 2015).

At Mount Etna, Middle Pleistocene faunal assemblages dated to >500 ka to ≥280 ka are interpreted as having occupied closed rainforest palaeoenvironments (QML1311H, QML1313) including taxa or lineages now only found in rainforests of northern Queensland and New Guinea (Hocknull, 2005; Hocknull *et al.*, 2007; Price & Hocknull, 2011; Cramb & Hocknull, 2010). A younger Middle Pleistocene fauna (QML1312) dated to 205–170 ka is interpreted as having occupied a xeric environment and includes species or lineages found in arid habitats today. The Late Pleistocene fauna (QML1456) from Capricorn Caves is interpreted to be more mesic in comparison to the xeric Middle Pleistocene fauna, but still drier-adapted than the older Middle Pleistocene rainforest fauna. Together, these three periods show major faunal transitions typified by local extinction and replacement of species with new more dry-adapted forms (Hocknull *et al.*, 2007; Price, 2012).

Phylogenetic analysis

A preliminary attempt was made to ascertain the phylogenetic position of the new fossil species of *Uromys* by scoring craniodental characters using a character state matrix first developed by Groves & Flannery (1994).

We restricted our assessment to the craniodental characters used by Groves & Flannery (1994) with the addition of one measurement character (Character 50: M^{1-3} length) and one measurement ratio (Character 51: M^{1-3} length/ M^1 width). These continuous data were binned and scored as multi-states for variable taxa. The length measurement was ordered in the analysis. All other characters were unordered. Three additional species, including the fossil taxon *U. aplini* sp. nov., *U. vika* (based on the description published by Lavery & Judge, 2017) and specimens considered to represent *U. sherrini* were used to augment the phylogenetic analysis (see Appendix 1). Only *U. siebersi* was not able to be scored, due to the rarity of specimens. Some character states were not able to be scored due to either their lacking in preservation in the fossils and extant craniodental remains, or obscurity in determining the state. Character states for 2–4, 8–9, 17, 20, 22, 44 could not be ascertained from comparison of specimens with character descriptions provided by Groves & Flannery (1994), so were given a “?” and considered uncertain. We have amended the character state of character 11 for *U. hadrourus* because it was incorrectly scored in Groves & Flannery (1994). All characters were weighted equally.

Molecular analysis by Bryant *et al.* (2011) found that *Melomys* is the sister taxon to *Uromys*, while *Paramelomys* is the sister clade to both genera. For this reason, we included *Paramelomys rubex* as the outgroup for the analysis to polarize the character states within *Uromys*. The modified matrix is shown in Table 1. The analysis was conducted using Mesquite version 3.61 (Maddison & Maddison, 2019) and PAUP 4.0 (Swofford, 2001).

Our phylogenetic assessment is only considered to be preliminary using standard parsimony, where the characters are polarized by an outgroup (*Paramelomys rubex*). Multi-state characters are considered to be polymorphic, whilst those characters with “?”s are considered to be uncertain. The tree-searching algorithm used was tree-bisection and reconnection (TBR) from 100 random additions. Bootstrap values were calculated using 1000 replicates, with the resulting nodes with values greater than 50% retained.

Abbreviations

QMF—Queensland Museum fossil specimen; QML—Queensland Museum fossil locality; QMJ, QMJM—Queensland Museum modern mammal specimen; CM—CSIRO Australian National Wildlife Collection mammal specimen; AM M.—Australian Museum mammal specimen; NMVC—Museum Victoria mammal specimen; ka (kilo annum)—thousands of years ago; Ma (mega annum)—millions of years ago.

Results

Two species of *Uromys* were identified from fossils in the study region, the extant *U. caudimaculatus* and the extinct *U. aplini* sp. nov. *Uromys caudimaculatus* was recovered from Capricorn Caves (QML1456) in excavation spits 142–147 cm, 152–157 cm, and 177–182 cm (inferred as dating to the Late Pleistocene), and *U. aplini* sp. nov. was recovered from multiple Middle Pleistocene deposits at Mount Etna.

Systematic palaeontology

Class Mammalia Linnaeus, 1758
 Subclass Theria Parker & Haswell, 1897
 Supercohort Placentalia Bonaparte, 1838
 Order Rodentia Bowdich, 1821
 Family Muridae Illiger, 1811
 Subfamily Murinae Illiger, 1811
 Tribe Hydromyini Alston, 1876 *sensu* Lecompte *et al.*, 2008

Uromys Peters, 1867

Synonyms: *Gymnomys* Gray, 1867; *Cyromys* Thomas, 1910; *Melanomys* Winter, 1983 (but see Jackson & Groves, 2015, for explanation).

Included species:

Uromys caudimaculatus (Krefft, 1867)
Uromys imperator (Thomas, 1888)
Uromys rex (Thomas, 1888)
Uromys porculus (Thomas, 1904)
Uromys anak Thomas, 1907
Uromys sherrini Thomas, 1923a
Uromys siebersi Thomas, 1923b
Uromys neobritannicus Tate & Archbold, 1935
Uromys hadrourus (Winter, 1984)
Uromys boeadii Groves & Flannery, 1994
Uromys emmae Groves & Flannery, 1994
Uromys vika Lavery & Judge, 2017

Generic diagnosis: Groves & Flannery (1994) considered three cranial characters (with the addition of one soft-tissue character) to be diagnostic of species of *Uromys*: a hard palate that extends posterior of the posterior margin of M³, I₁ is much deeper than it is wide, and a greatly expanded anterolateral spine on the auditory bulla.

Uromys caudimaculatus (Krefft, 1867)

Fig. 3A, 3B

Material examined. QML1456: spit 142–147 cm: QMF60126 right M¹, QMF60127 left M¹, QMF60128 right M¹, QMF60129 left M², QMF60130 left M₁, QMF60131 right M₂. Additional specimens were also recovered from spits 152–157 cm, and 177–182 cm.

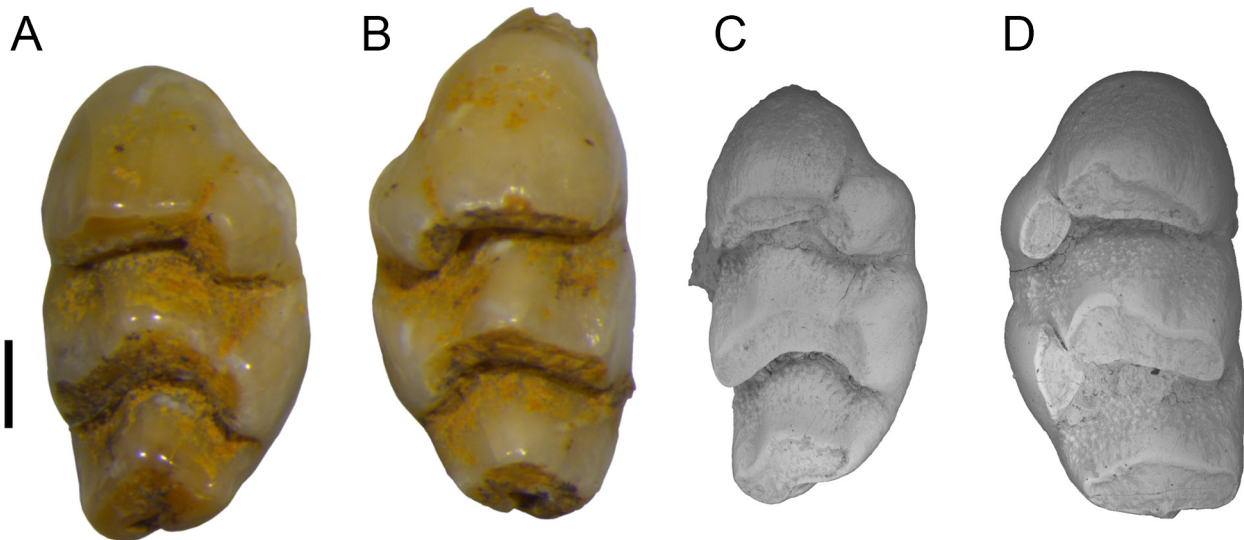


Figure 3. Succession of *Uromys* spp. in the Mt Etna area. (A–B) *Uromys caudimaculatus*, (A) QMF60126 right M¹, QML1456 spit 142–147, c. 50 ka; (B) QMF60127 left M¹, deposit and age as for A. (C–D) *Uromys aplini*, (C) QMF55340 left M¹, QML1312, 205–170 ka; (D) QMF60125 right M¹, QML1311 H, > 450 ka. Scale bar = 1 mm.

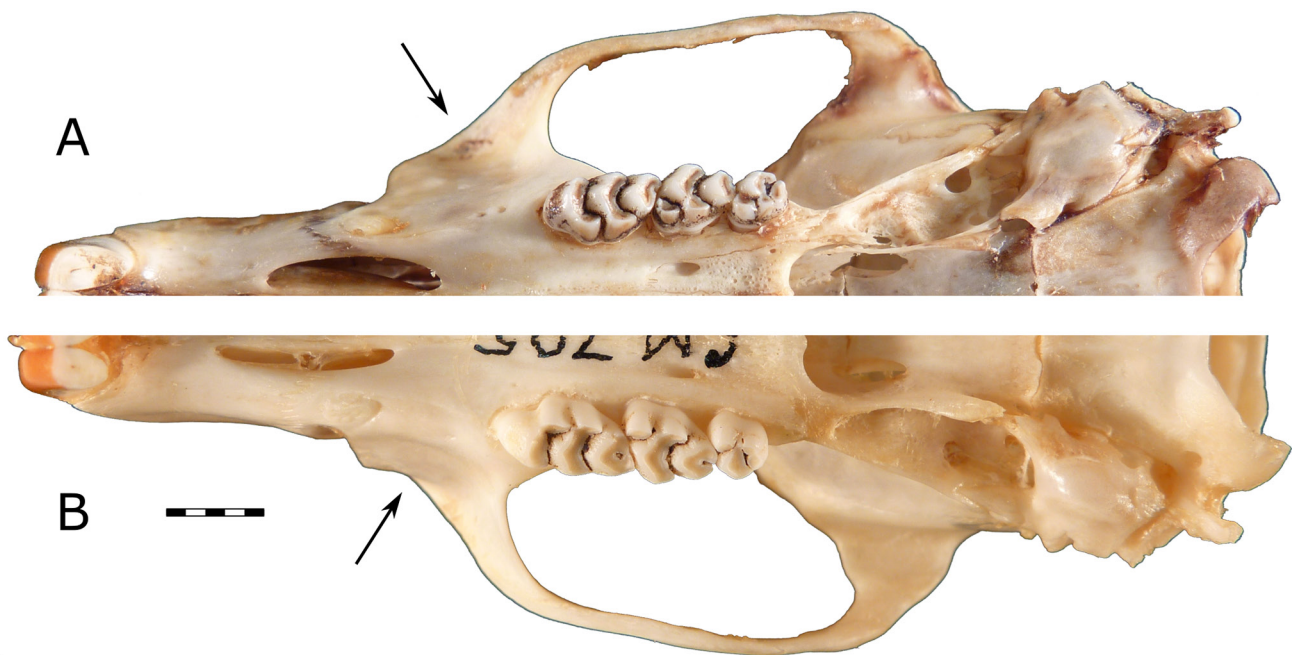


Figure 4. Comparison of skulls of *Uromys sherrini* and *U. caudimaculatus* in ventral outline. (A) *U. sherrini* (CM10822); (B) *U. caudimaculatus* (CM705). The larger degree of deflection in the zygomatic plate, seen in *U. caudimaculatus*, is indicated with an arrow. Scale bar = 5 mm.

Remarks. Isolated molars of this species are distinguished by a combination of characters including very large size; crescentic lophs on M^{1-2} ; deep posterior indent present on M^{1-2} ; long, variably bifurcated lingual root on M^{1-2} ; crescentic lophs on M_{1-2} ; lingual root present on M_1 ; large posteroconid on M_{1-2} ; and a relatively shallow cleft between the antero-buccal cuspid and protoconid on M_1 .

Uromys caudimaculatus was previously considered to include *U. sherrini*, so it is pertinent to include a list of characters that distinguish these species. These are: the margins of the interorbital area above the orbits, which are almost parallel in *U. sherrini* but divergent in *U. caudimaculatus* (Thomas, 1923a); the anterior palatal foramina are commonly broader in *U. sherrini*; the M^{1-2} of *U. sherrini* have shallower posterior indents on the T8–9 complex; the posterior loph on $M^{3/3}$ is commonly narrower; the nasals are shorter, not projecting anterior of the premaxillae as in *U. caudimaculatus*; the anterior edge of the zygomatic plate is directed antero-lingually in dorsal or ventral outline, while that of *U. caudimaculatus* is deflected, making it parallel with the rostrum (Fig. 4).

Specimens of *U. caudimaculatus* from QML1456 have only slightly worn tooth crowns, indicating that the owls thought to be the accumulating agents of the deposit were preying on young individuals. The excavation spit that yielded the stratigraphically youngest *U. caudimaculatus* specimens (i.e., 142–147 cm) is probably slightly younger than 50 kyr (see Price *et al.*, 2015 for a full discussion of the age of the deposit). The older spits (i.e., 152–157 cm and 177–182 cm) are undated, but are likely to be Late Pleistocene (c. 80–60 ka) based on the age model presented in Price *et al.* (2015). Deposition in QML1456 is thought to have been continuous during the late Quaternary, with no evidence of depositional hiatuses.

Uromys aplini sp. nov.

urn:lsid:zoobank.org:act:C52317A8-D118-4E10-AA9C-21DF62C8EECA

Figs 3C, 3D, 5–7

Holotype. QMF52014 (Queensland Museum fossil specimen) partial skull, QML1313 (Queensland Museum fossil locality) Speaking Tube Cave, Mount Etna, eastern central Queensland. Deposit has a minimum age of c. 280 ka (Hocknull *et al.*, 2007). **Paratypes.** QMF55753 partial skull; QMF55542 right mandible with M_1 ; both specimens have same locality as holotype, QML1313.

Material examined. QML1311H: QMF55547 right M^1 , QMF55548 right M^2 , QMF55549 right M^3 , QMF55550 left M_1 , QMF55551 right M_1 , QMF55552 left M_3 , QMF60125 right M^1 ; QML1313: QMF52014 partial skull, QMF55522 left M^1 , QMF55523 left M^1 , QMF55524 right M^1 , QMF55525 left M^2 , QMF55526 right M^2 , QMF55527 right M^2 , QMF55528 right M^3 , QMF55529 left M^3 , QMF55530 left M^3 , QMF55531 left M_1 , QMF55532 left M_1 , QMF55533 left M_1 , QMF55534 right M_2 , QMF55535 left M_2 , QMF55536 left M_2 , QMF55537 right M_3 , QMF55538 left M_3 , QMF55539 left M_3 , QMF55540 left I^1 , QMF55541 left maxilla fragment, QMF55543 right mandible with M_1 and M_3 , QMF55544 right M^3 ; QML1313A: QMF55545 left M^1 , QMF55546 right M_1 ; QML1312: QMF55340 left M^1 . Additional specimens were also recovered from QML1284, QML1284A, QML1311C/D, QML1311J, QML1383, QML1384LU, and QML1385.

Age Range. Chibanian (Middle Pleistocene), chronometrically dated to >500 ka to c. 205 ka.

Diagnosis. Large *Uromys*, but smaller than most species of *Uromys* (*Uromys*) with the exception of *U. hadrourus* (Fig.

Table 2. Craniodental measurements of *Uromys aplini* sp. nov. All measurements in millimetres. SD = standard deviation; CV = coefficient of variation; APF = anterior palatal foramen; QML = Queensland Museum Locality.

	QML	<i>n</i>	mean	SD	range	CV		<i>n</i>	mean	SD	range	CV
I ¹ depth	1313	3	3.05	0.07	2.98–3.11	—	I ¹ width	3	1.64	0.05	1.58–1.68	—
interorbital width	1313	2	8.58	0.33	8.34–8.81	—	zygomatic plate length	2	7.40	0.79	6.84–7.96	—
APF length	1313	2	6.29	0.41	6.00–6.58	—	diastema length	2	14.55	0.07	14.50–14.60	—
hard palate length	1313	2	25.97	0.79	25.40–26.53	—	hard palate width	2	10.03	0.07	9.98–10.08	—
I ₁ depth	1313	1	1.98	na	na	na	I ₁ width	2	1.38	0.35	1.13–1.63	—
M ¹ length	1311 H	1	4.82	na	na	na	M ¹ width	1	2.57	na	na	na
	1313	3	5.09	0.20	4.86–5.42	—		4	2.84	0.22	2.53–3.02	—
	1313A	—	—	—	—	—		2	2.82	0.12	2.73–2.90	—
	1312	1	5.27	na	na	na		1	2.85	na	na	na
	all	5	5.08	0.26	4.82–5.42	—		8	2.80	0.18	2.53–3.02	—
M ² length	1311 H	1	3.33	na	na	na	M ² width	1	2.78	na	na	na
	1313	6	3.71	0.21	3.46–4.00	—		7	2.83	0.12	2.71–3.04	—
	1313A	—	—	—	—	—		1	2.72	na	na	na
	all	7	3.66	0.24	3.33–4.00	—		9	2.81	0.11	2.71–3.04	—
M ³ length	1311 H	2	2.38	0.07	2.33–2.43	—	M ³ width	2	2.13	0	2.13–2.13	—
	1313	6	2.26	0.15	2.08–2.52	—		6	2.08	0.12	1.92–2.21	—
	all	8	2.29	0.14	2.08–2.52	—		8	2.09	0.10	1.92–2.21	—
M ¹⁻³ length	1313	2	10.17	0.29	9.96–10.37	—	M ₁₋₃ length	3	10.74	0.24	10.48–10.95	—
M ₁ length	1311 H	4	4.15	0.17	3.96–4.33	—	M ₁ width	4	2.62	0.08	2.55–2.73	—
	1313	6	4.43	0.13	4.19–4.54	—		6	2.67	0.18	2.37–2.93	—
	1313A	2	4.17	0.09	4.10–4.23	—		2	2.55	0.12	2.46–2.63	—
	all	12	4.29	0.19	3.96–4.54	4.46		12	2.63	0.14	2.37–2.93	5.50
M ₂ length	1311 H	4	3.51	0.14	3.42–3.72	—	M ₂ width	5	2.85	0.11	2.69–2.97	—
	1313	3	3.45	0.28	3.19–3.74	—		3	2.81	0.09	2.70–2.89	—
	1313A	3	3.31	0.14	3.23–3.47	—		3	2.68	0.08	2.61–2.77	—
	all	10	3.43	0.19	3.19–3.74	5.51		11	2.79	0.12	2.61–2.97	4.14
M ₃ length	1311 H	2	3.01	0.26	2.82–3.19	—	M ₃ width	2	2.48	0.01	2.47–2.48	—
	1313	4	2.65	0.16	2.45–2.78	—		4	2.29	0.12	2.18–2.43	—
	all	6	2.77	0.25	2.45–3.19	—		6	2.35	0.13	2.18–2.48	—

8; Table 2); it is distinguished on the following combination of characters: posterior indent on T8–9 of M¹⁻² poorly developed; molar enamel ornament moderately developed; anterior palatal foramina short, shared equally between premaxilla and maxilla; rostrum proportionally short and robust; supraorbital ridges and postorbital processes absent. Features that further distinguish *U. aplini* from all other species of *Uromys* are listed in the Remarks section.

Groves & Flannery (1994) divided *Uromys* into two subgenera: *U. (Uromys)* and *U. (Cyromys)*. *Uromys aplini* is placed in *U. (Uromys)* on the basis of the following diagnostic characters identified by Groves & Flannery (1994): short, slit-like anterior palatal foramina; simplified, elongate molars; reduced M^{3/3}; posteriorly lengthened bony palate; reduced anterior lophid on M₁, which fuses to middle lophid after moderate wear; zygomatic arches swing posteriorly and ventrally to level of molar alveoli; and orthodont incisors.

Etymology: Named for Kenneth Peter Aplin (1958–2019), for his contribution to Australian palaeontology and the taxonomy and systematics of Australasian murids.

Description

Skull. Two partial skulls are known (QMF52014 and 55753, Fig. 5A,B). The lacrimals, jugals, and much of the posterior of the skull and basicranium are missing from both specimens.

The nasals appear to be consistent in width along preserved length, tapering sharply at posterior contact with frontals.

Premaxilla short and robust. Anterior palatal foramen short, narrow, tapering abruptly at extremities, occupying similar area of premaxilla and maxilla. Anterior palatal foramen roughly half of length anterior of M¹. Narrow crest on ventral surface of maxilla between junction with premaxilla and anterior margin of M¹ variably

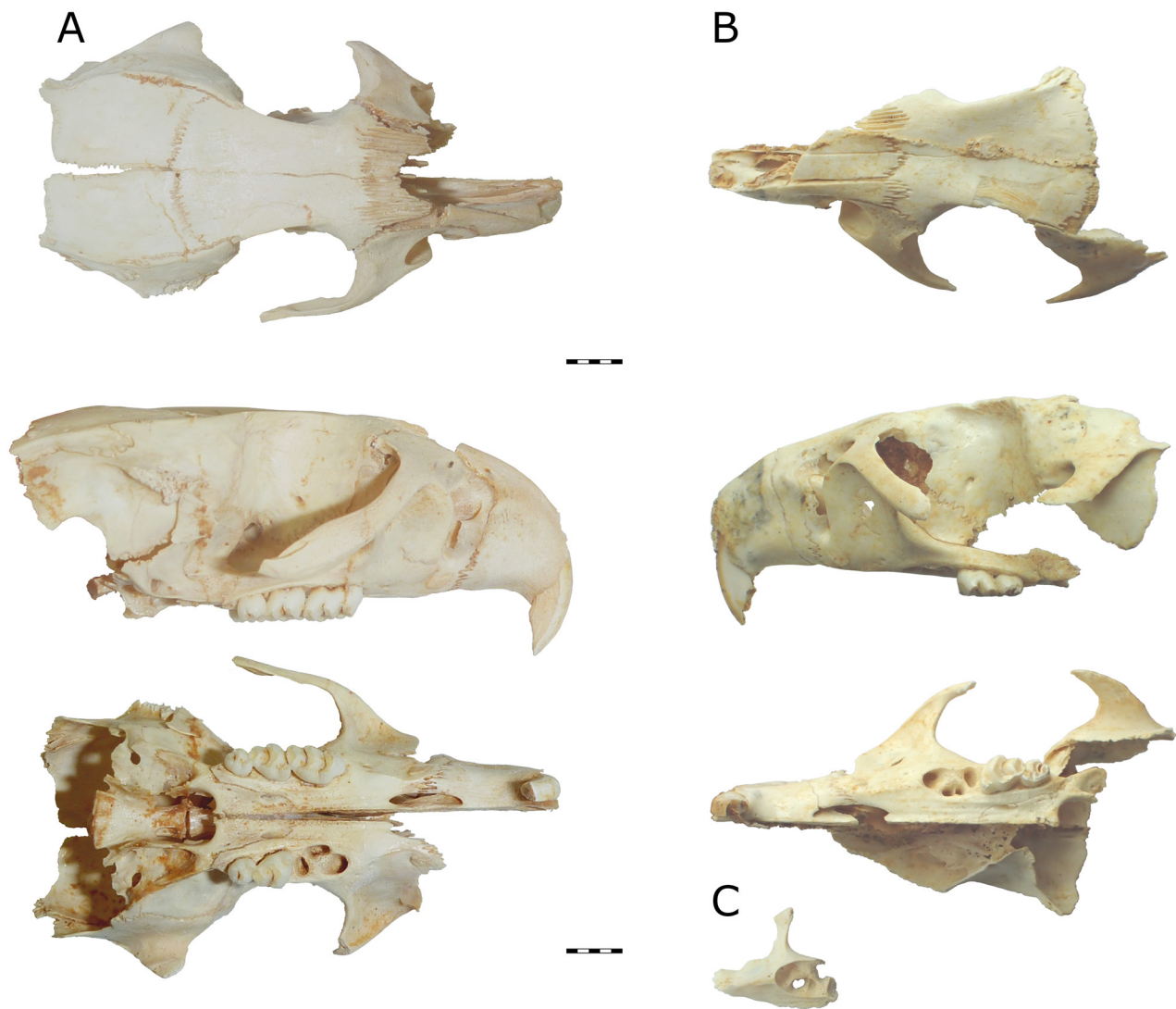


Figure 5. Cranial elements of *Uromys aplini* sp. nov. (A) QMF52014 partial skull in (top to bottom) dorsal, right lateral, and ventral view; (B) QMF55753 partial skull in dorsal, left lateral, and ventral view; (C) QMF55541 left maxilla fragment, showing a narrow crest on the diastema. Scale bar = 5 mm.

developed, likely associated with age (some specimens, e.g., QMF55541, have it developed to an extreme degree, forming a blade. Fig. 5C). Zygomatic plate long, anterior edge straight, evenly curving posteriorly at dorsal end into zygomatic arch. Maxillary portion of zygomatic arch slopes posteroventrally at approximately 45° angle, almost reaching level of molar alveoli.

Palatine contacts maxilla level with posterior margin of M^1 . Posterior palatal foramen level with M^2 . Palate terminates in small, blunt postpalatal spine, approximately level with most posterior point of maxilla.

Frontals with sharp corner between temporal and orbital faces. Very small postorbital processes on squamosals, not associated with sutures. Supraorbital ridges not evident on frontals; parietal crests weakly developed on dorsal margin of squamosals and parietals. Braincase not greatly inflated, relatively flat dorsally, width exaggerated on QMF52014 by parting of parietals at midline.

I^1 . Proportionally deep (I^1 depth/width of QMF52014 =

2.98/1.66 mm), orthodont. One paratype (QMF55753, Fig. 5B) appears to retain orange pigment in enamel, although this may instead be diagenetic iron staining.

M^1 . Crown elongate, rounded anterior margin and angular posterior margin. Lophs sloped posteriorly. Accessory cusp and anterior cingulum absent. Lingual cusps bulge lingually at bases, giving lingual margin of crown an irregular appearance. Buccal cusps do not bulge at bases. T1 oval-shaped in occlusal outline, oriented antero-buccally postero-lingually. T1 postero-lingual of T2. T1 separated from T2 by shallow cleft; T1 and T2 join after moderate wear. T2 broad and robust. T3 directly buccal of T2, posterior margins of T2–3 form straight line. T3 small, fused to T2. T3 discernible from T2 by shallow, poorly defined groove on anterior face of T2–3 complex. T4 subcircular in occlusal outline when unworn, becomes subtriangular after wear. In occlusal outline, T4 projects to a point anterior of the junction with T5; tapers posteriorly. T4 tapers towards T5, separated by a shallow cleft, joined after moderate wear. T5

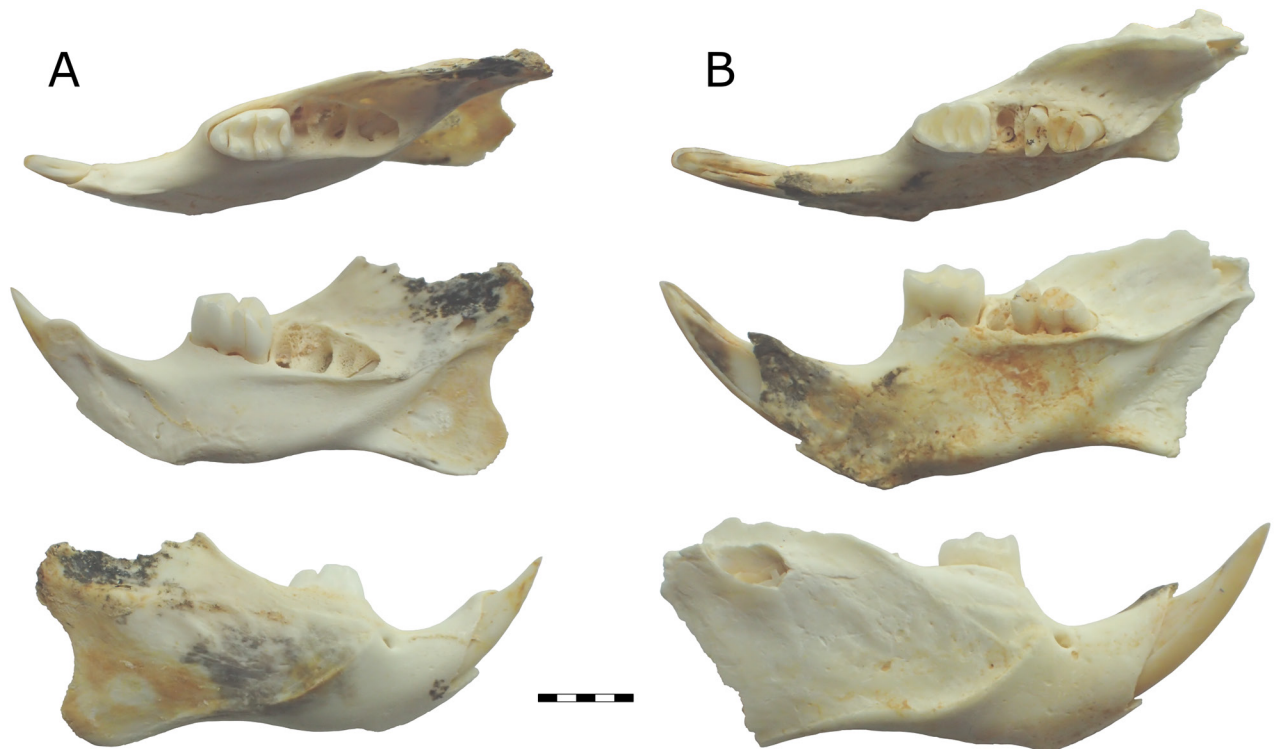


Figure 6. Mandibles of *Uromys aplini* sp. nov. (A) QMF55542 right mandible with M_1 ; (B) QMF55543 right mandible with M_1 , partial M_2 , and M_3 . Scale bar = 5 mm.

broad, boomerang-shaped in occlusal outline, with bulk of T5 antero-buccal of T4 and antero-lingual of T6. T6 poorly defined, variably separated from T5 by shallow groove on anterior face of T5–6 complex. T6 broad, oriented antero-lingually postero-buccally, continuous with buccal half of T5. T5–6 complex roughly parallel with T8–9 complex. T7 appears absent, although one specimen (QMF55522, Fig. 7C) has a bulge in the posterior loph that could be interpreted as a T7 fused to T8. T8–9 complex broad, based between buccal margin of crown and posterior point of T4. T9 fused to T8, poorly defined by change in angle of anterior margin of occlusal surface of T8–9 complex. Very small posterior indent associated with posteroloph, commonly not visible in occlusal view.

Fine enamel ornament present on anterior faces of all lochs. M^1 has four roots: anterior, two lingual (commonly fused close to crown), and postero-buccal. Molar roots commonly split into multiple rootlets at tips. Alveoli of lingual roots variably fused, creating appearance of a single elongate lingual root.

M^2 . Elongate, tapering posteriorly. Lingual cusps bulge lingually at bases, buccal cusps do not. T1 forms antero-lingual corner of crown. T1 subcircular in occlusal outline when slightly worn, becomes subtriangular (tapering buccally and posteriorly) after wear. T2–3 absent. Position of T3 variably marked by shallow depression on anterior face of T5–6 complex. T4 directly posterior of T1. T4–6 loph essentially identical to that on M^1 . T8–9 complex based between buccal margin of T6 and posterior point of T4. T8–9 tapers slightly but does not form a point. T8 and T9 not differentiated.

A ridge on the lingual side of T8 may represent a T7. Very small posterior indent associated with posteroloph, commonly not visible in occlusal view. Fine enamel ornament on anterior faces of both lochs, possibly less developed than that on M^1 . M^2 has four main roots: antero-buccal, postero-buccal, postero-lingual, and antero-lingual. The antero-lingual and postero-lingual roots are variably joined. The antero-buccal root is variably bifurcated at the tip into two small rootlets.

M^3 . Compact and simplified, moderately reduced. Some specimens (e.g., QMF55528, Fig. 7H) subcircular in occlusal outline. T1 well defined, rounded, oval-shaped in occlusal outline. T2–3 absent. Individual cusps of T4–6 loph not discernible. T4–6 loph gently curved, most anterior point at presumed location of T5. T4–6 loph sloped posteriorly. Posterior cusp broad, slightly narrower than T4–6 loph. Posterior cusp upright, very close to T4–6 loph. Some specimens (e.g., QMF55530, Fig. 7G) have posterior cusp very close to “T4” but larger gap separating posterior cusp from “T6”. Posterior cusp oval-shaped in occlusal outline. One specimen (QMF55544) has a small posterior cingulum cusp. M^3 has four roots: antero-buccal, posterior, and joined antero-lingual and lingual.

Mandible. No specimens are completely intact, with all displaying degrees of damage to the posterior processes and incisor alveolus. Mandible deep and robust, with deepest point ventral of M_1 . M_1 longer than M_2 , but similar width. M_3 smaller than M_2 , but not heavily reduced. Coronoid process damaged or missing on all specimens, but appears to be taller than articular process. Articular process projects slightly posterior of angular process. Angular process damaged on

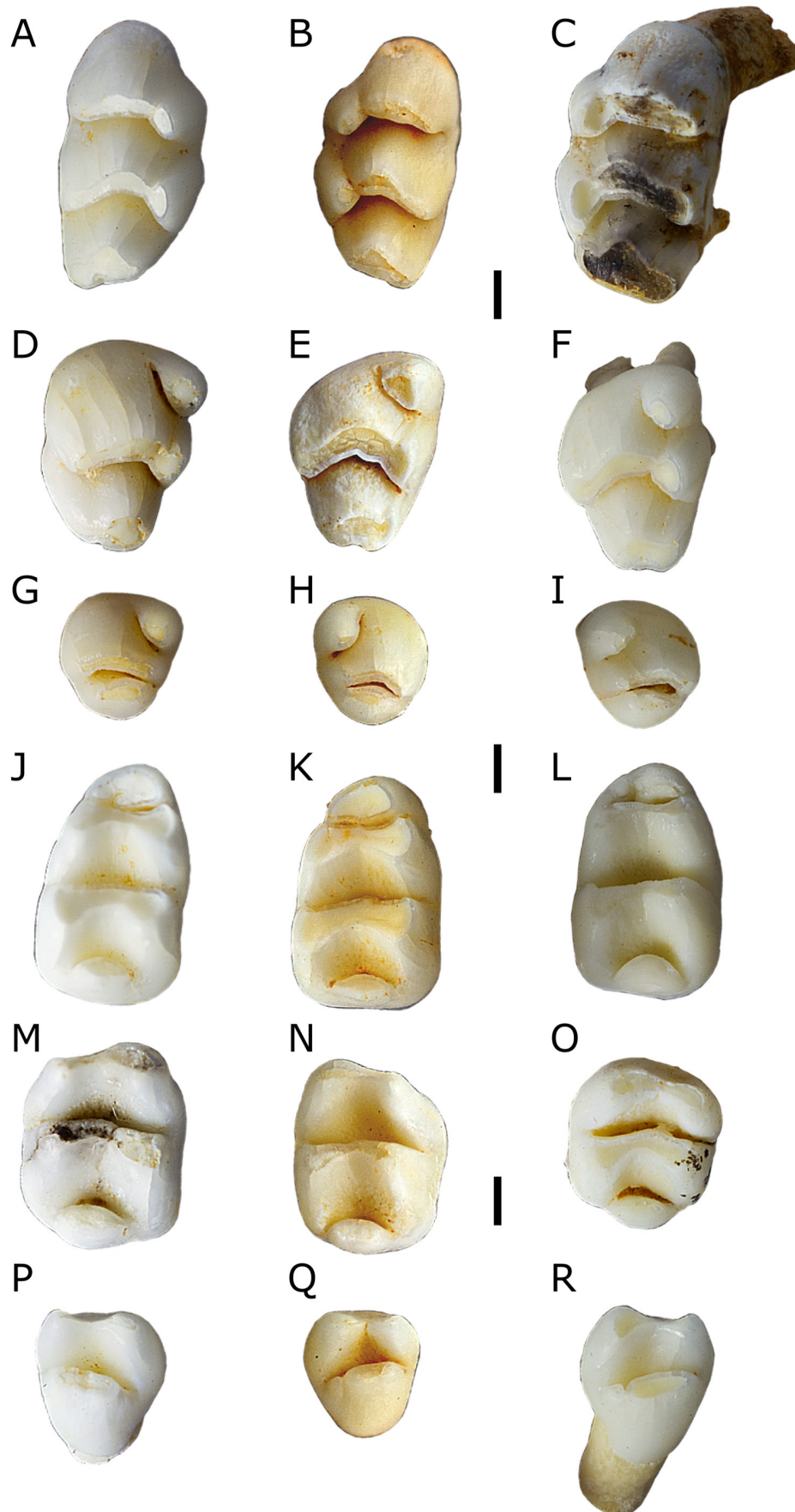


Figure 7. Isolated molars of *Uromys aplini* sp. nov. (A) QMF55524 right M¹; (B) QMF55523 left M¹; (C) QMF55522 left M¹; (D) QMF55527 right M²; (E) QMF55525 right M²; (F) QMF55526 right M²; (G) QMF55530 right M³; (H) QMF55528 left M³; (I) QMF55529 left M³; (J) QMF55531 left M₁; (K) QMF55533 left M₁; (L) QMF55532 left M₁; (M) QMF55534 right M₂; (N) QMF55536 left M₂; (O) QMF55535 left M₂; (P) QMF55537 right M₃; (Q) QMF55539 left M₃; (R) QMF55538 left M₃. Scale bar = 1 mm.

all specimens, but appears to be rounded. Mental foramen ventral of dorsal inflexion of diastema. Superior masseteric crest very poorly defined below molars; inferior masseteric crest well developed, terminates anteriorly posterior of mental foramen. Mandibular symphysis marked by dorsal crest in anterior part of diastema; symphysis ends ventrally of anterior root of M_1 . Incisor alveolus forms prominent tubercle on buccal surface of ascending ramus, although this is damaged in all specimens. Postalveolar ridge sharply defined below and posterior of M_3 , less defined posterior of retromandibular fossa. Retromandibular fossa small in young adult individuals, greatly expanded in mature individuals (assessed on the basis of molar wear).

I₁. Proportionally deep (I_1 depth/width of QMF55542 [subadult] = 1.98/1.13, adults proportionally deeper). One specimen (QMF55543, Fig. 6B) may retain orange pigment in enamel, but lost in majority of specimens.

M₁. Rounded anteriorly, subrectangular posteriorly. Anterior and middle lophids crowded together. Anterior lophid upright, middle, and posterior lophids sloped anteriorly. Anterior lophid narrower than middle lophid. Middle and posterior lophids of similar width. Antero-buccal cuspid small, subcircular in occlusal outline, fused to antero-lingual cuspid. Antero-buccal and antero-lingual cuspids only distinguishable when unworn, form single anterior lophid after moderate wear. Antero-lingual cuspid much larger than antero-buccal cuspid, forms much of the anterior lophid. Unworn specimens show antero-lingual cuspid with two buccal extensions: one joining the antero-buccal cuspid, the other directly posterior and postero-lingual of the antero-buccal cuspid between the main body of the anterior lophid and the middle lophid. Antero-buccal cuspid separated from protoconid by shallow cleft, eliminated by wear on some specimens; antero-lingual cuspid separated from metaconid by relatively deeper cleft, more resistant to wear.

Protoconid subtriangular in occlusal outline, tapering linguallly to join metaconid and posteriorly along buccal margin of crown. Metaconid subequal in size to protoconid. Metaconid subtriangular in occlusal outline, tapering buccally to join protoconid, tapering slightly posteriorly and anteriorly. Anterior margin of middle lophid buccally perpendicular to long axis of crown, curves antero-lingually to most anterior point of metaconid. Posterior face of middle lophid curved, bowing anteriorly between most posterior points of protoconid and metaconid.

Entoconid directly posterior of metaconid. Entoconid subtriangular in occlusal outline, tapering buccally to join hypoconid and posteriorly to a lesser degree. Hypoconid directly posterior of protoconid, buccal and slightly posterior of entoconid. Hypoconid subtriangular in occlusal outline, tapering linguallly to join entoconid, and posteriorly to a lesser degree. Hypoconid and entoconid variably have small anterior extensions. Hypoconid projects slightly further posteriorly than entoconid. Anterior edge of occlusal surface of posterior lophid commonly straight, but some specimens (e.g., QMF55533, Fig. 7K) have a slight bulge, at approximately the midline of the crown. Posterior margin of occlusal surface curved, bowed anteriorly with most anterior point directly posterior of midline junction between hypoconid and entoconid. Posteroconid tolerably well

developed, lenticular in occlusal outline, bound by bases of hypoconid and entoconid. Posteroconid does not project beyond posterior margin of crown. Fine enamel ornament on posterior faces of middle and posterior lophids, not visible on anterior lophid due to close proximity of middle lophid. M_1 has three roots: anterior, a broad posterior, and a small lingual root.

M₂. Crown roughly square in occlusal outline, with rounded corners. Both lophids sloped anteriorly. Protoconid larger than metaconid, both at apex and base. Protoconid tear-shaped in occlusal outline, tapering linguallly to join metaconid at midline of crown. Metaconid directly lingual of protoconid, tear-shaped in occlusal outline, tapering buccally. Unworn specimens (e.g., QMF55536, Fig. 7N) have no cleft separating protoconid and metaconid. Hypoconid directly posterior of protoconid. Hypoconid tear-shaped when unworn, becomes subtriangular after light wear. Hypoconid tapers antero-lingually to join entoconid at midline of crown. Hypoconid tapers posteriorly further than entoconid. Entoconid slightly less robust than hypoconid. Entoconid tear-shaped in occlusal outline, tapering directly buccally, meeting hypoconid at an angle. No separation between hypoconid and entoconid.

Posteroconid well developed, lenticular in occlusal outline. Posteroconid commonly centred on midline of crown, although one specimen (QMF55535, Fig. 7 O) has it centred slightly buccal of the midline. Posteroconid projects slightly beyond posterior margin of crown. Fine enamel ornament on posterior faces of lophids. M_2 has two broad roots: anterior and posterior.

M₃. Almost triangular in occlusal outline, with heavily rounded corners. Protoconid slightly larger than metaconid. Protoconid tear-shaped in occlusal outline, tapering linguallly to join metaconid. Metaconid tear-shaped in occlusal outline, tapering buccally to join protoconid. Protoconid and metaconid joined by narrow ridge. Posterior lophid broad, commonly supplemented by small cuspid on buccal side. Posterior lophid shaped like an elongate oval in occlusal outline, supplementary cuspid subcircular. Supplementary buccal cuspid variably separated from posterior lophid by shallow cleft or fused. M_3 has three roots: posterior, and fused antero-buccal and antero-lingual.

Remarks

Uromys aplini can be distinguished from other members of *Uromys* (*Uromys*) as follows: *Uromys aplini* differs from *U. caudimaculatus* by being smaller; having a less elongate rostrum; having a smaller posterior indent in T8–9 on M^{1-2} ; and having shorter anterior palatal foramina. *Uromys aplini* differs from *U. sherrini* by being smaller; having a less elongate rostrum; and having a more reduced $M^{3/3}$. *Uromys aplini* differs from *U. hadrourus* by being larger; having proportionally shorter anterior palatal foramina; having a proportionally shorter rostrum; by commonly possessing a crest on the maxilla between the maxilla/premaxilla contact and M^1 ; and having a zygomatic arch that plunges further ventrally, reaching the level of the molar alveoli. The molars of *Uromys aplini* could not be effectively compared to those of *U. hadrourus*, as all examined specimens of the latter were heavily worn. *Uromys aplini* differs from

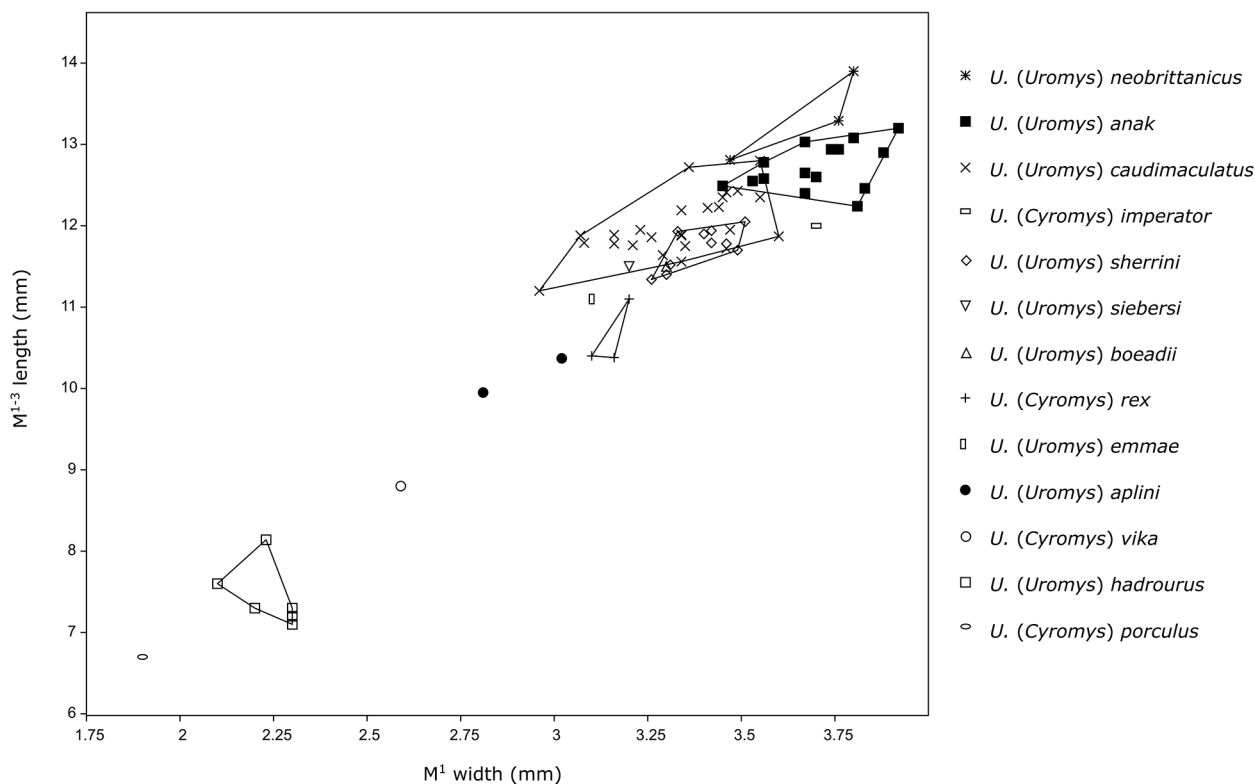


Figure 8. Bivariate plot of molar proportions (M¹ width vs M¹⁻³ length, in mm) of species of *Uromys*. Additional data provided by Tate (1951), Winter (1984), Groves & Flannery (1994) and Lavery & Judge (2017). Plot generated in PAST 2.12 (Hammer *et al.*, 2001).

U. anak by being smaller; having a less elongate rostrum; lacking postorbital processes; having a smaller posterior indent in T8–9 on M¹⁻²; and having the anterior palatal foramina shared equally between the premaxilla and maxilla. *Uromys aplini* differs from *U. neobritannicus* by being smaller; lacking large postorbital processes; having the skull relatively flat dorsally; and having parietals that are roughly rectangular in dorsal outline. *Uromys aplini* differs from *U. emmae* by being smaller; having a deeper zygomatic arch; having the zygomatic plate not projecting as far anterior of the zygomatic arch; and having the anterior palatal foramina shared equally between the premaxilla and maxilla. *Uromys aplini* differs from *U. boeadii* by being smaller; having smaller postorbital processes; and lacking supraorbital ridges.

Only one skull of *U. siebersi* is known, and this specimen was not available for the current study. But a measurement of the molar row (13.3 mm) provided by Groves & Flannery (1994) shows that *U. siebersi* is larger than *U. aplini* in this aspect (Table 2). Thomas (1923b) also provided measurements, though these are less precise than currently obtainable with modern precision measuring tools. The interorbital width and length of the “palatal foramina” (presumably the anterior palatal foramina) are both larger (10.3 mm and 7 mm, respectively, versus 8.34 mm and 6.00 mm for *U. aplini*).

Uromys aplini is hitherto known mostly from deposits at Mount Etna that are dominated by taxa that had ecological affinities to rainforest environments. The oldest deposits that yield the species are >500 ka, whilst the youngest is 205–170 ka.

Phylogenetic analysis

Our phylogenetic analysis returned topological features similar to that recovered by Groves & Flannery (1994). We used *Paramelomys rubex* as the most appropriate outgroup taxon to polarize the character-states within *Uromys*. Thirty-three characters were parsimony informative with seven uninformative and considered to be autapomorphies of these taxa. The derived character states for characters 12, 24 and 25 are considered to be autapomorphies of *U. rex*, so are uninformative in relation to *U. aplini*. The derived character states for characters 34 and 38 are considered to be autapomorphies of *U. imperator* and *U. emmae* respectively, also uninformative for the fossil taxon. Finally, uninformative characters 15 and 37 are restricted to *U. hadrourus*, with the derived state of character 15 an autapomorphy and 37 ambiguous due to the missing states in the fossil taxon (*U. aplini*) and in *U. sherrini*.

The parsimony analysis returned two most parsimonious trees (MPT) of 93 steps (Fig. 9). Both MPTs consistently returned a basal split with one clade solely composed of species within the subgenus *Cyromys* and found today in the Solomon Islands group (*U. imperator*, *U. rex*, *U. porculus*, and *U. vika*). The *Cyromys* clade is strongly supported by bootstrap value of 91%. The other clade is composed solely of species within the subgenus *Uromys* and includes our fossil taxon, *U. aplini*. Although this clade is poorly supported, it is likely that the large amount of missing data and morphological variability of *U. caudimaculatus* have created internal instability within this clade. Further characterization of *U. caudimaculatus* subspecies and better

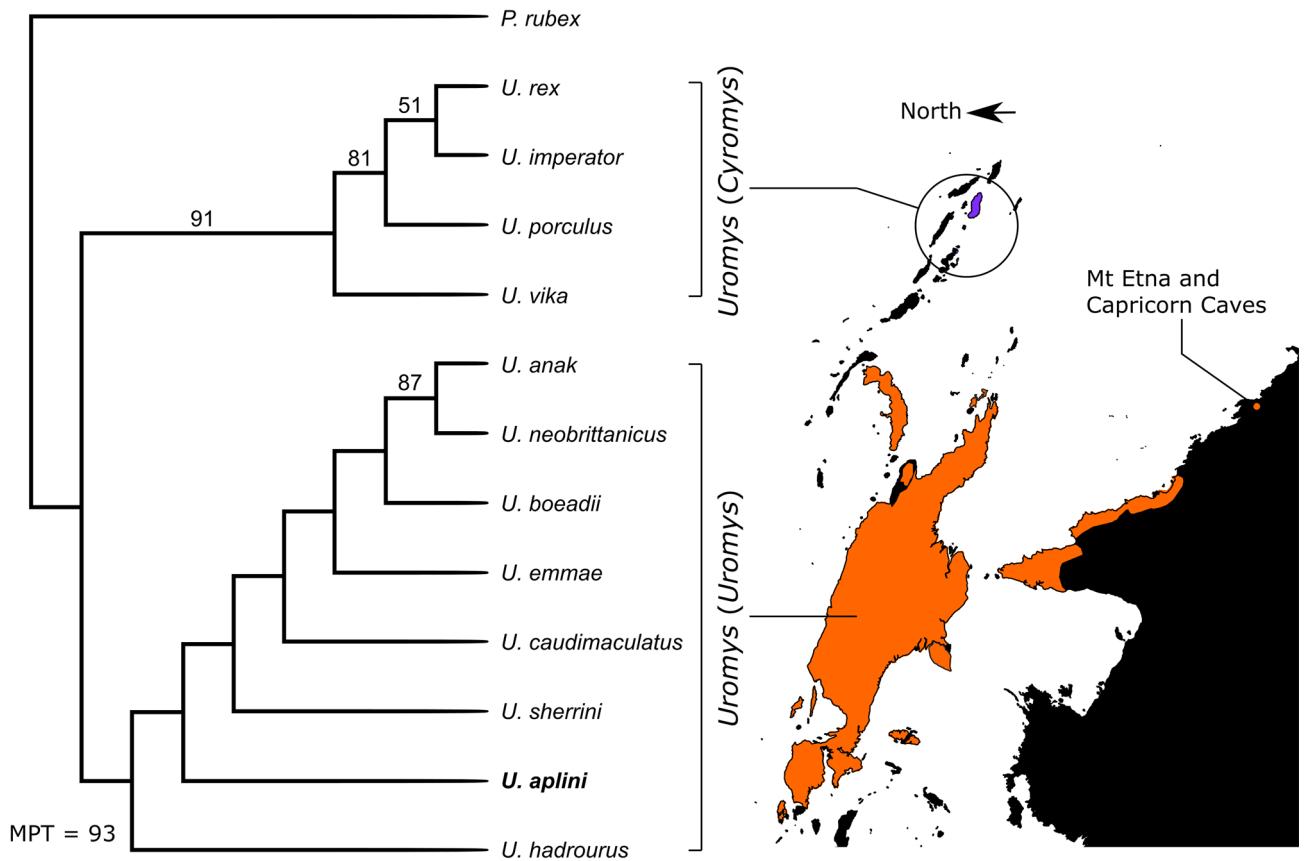


Figure 9. Results of preliminary phylogenetic analysis using parsimony. Bootstrap values > 50% provided showing monophyly of the Solomon Islands *Uromys* (*Cyromys*) and Australopapuan clade as sister taxon with Australian species basal to New Guinean species.

resolution of missing data may increase the support for the monophyly of *Uromys* (*Uromys*) and *Uromys* (*Cyromys*).

Resolution within the *Uromys* (*Uromys*) clade is poor, although the New Guinean *U. anak* and New Britain *U. neobritannicus* are strongly supported (87%) as sister taxa. The positions of the remaining taxa are poorly supported by bootstrap values, but both MPTs return identical positions of all species, suggesting that the overall topology is valid. At the base of the clade lie the Australian *Uromys hadrourus*, the fossil taxon *U. aplini*, and *U. sherrini*. In a more derived position, sister to these Australian endemic species, is *U. caudimaculatus*, which is then sister taxon to a clade containing the northern New Guinean island endemics (*U. emmae* and *U. boeadii*), the mainland New Guinea *U. anak*, and *U. neobritannicus* from New Britain.

The two basal clades, comprising *Uromys* (*Cyromys*) and *Uromys* (*Uromys*), were supported by Groves & Flannery (1994), so this result is not surprising. But our analysis, using *Paramelomys* as the outgroup, suggests that the Australian *Uromys* are basal to the *Uromys* (*Uromys*) clade.

The Middle Pleistocene age of our phylogenetically basal extinct taxon (*U. aplini*) is younger than the divergence time estimates (e.g., Early Pleistocene) for the more derived extant species within the clade (Watts & Baverstock, 1994; Bryant *et al.*, 2011). This would probably preclude *U. aplini* from being a chronospecies of the extant Australian species of *Uromys* (*Uromys*).

Discussion

Phylogeny and biogeography of *Uromys*

Our phylogenetic analysis supports three extant species of *Uromys* in northern Queensland, including two that are geographically restricted (*U. hadrourus* and *U. sherrini*) and one that is more broadly distributed across the northern region of Cape York (*U. caudimaculatus*). Fossils described here demonstrate that species of *Uromys* were previously more widespread in northeastern Australia than would be expected on the basis of their present distribution. Importantly, they show that *Uromys* occurred in regions during the Pleistocene that are today south of major modern biogeographic barriers for mesic taxa (e.g., the Burdekin and St Lawrence Gaps, see Bryant & Krosch, 2016).

The Middle Pleistocene extinct species *U. aplini* is phylogenetically positioned near the base of the *Uromys* (*Uromys*) clade between the geographically and ecologically restricted *U. hadrourus* and *U. sherrini* (Fig. 9). All taxa are found in northern Queensland, along the eastern seaboard. These taxa do not, however, form a resolved clade to the exclusion of species from New Guinea and its surrounding islands; therefore, it is hard to determine whether the Australian species are a monophyletic clade suggesting a single arrival and diversification. A reading of the current preliminary phylogenetic hypothesis would have the ancestor of *Uromys* dispersing from the Indo-New Guinea region

and founding two, possibly parallel radiations that derive *Uromys* (*Uromys*) and *Uromys* (*Cyromys*). One lineage either diversified from isolation within, or has become restricted to, the Solomon Islands group, producing all of the members of *Uromys* (*Cyromys*) and their current biogeographic distribution. The other, arriving on mainland Australia, diversified first and then dispersed to the islands and mainland New Guinea with the most derived taxon reaching New Britain.

The Pleistocene record of *U. aplini* demonstrates that *Uromys* was present in Australia over 500,000 years ago, and occurred well south of the current biogeographical range of the genus, reaching at least the Mount Etna region by the Middle Pleistocene. Molecular-based data estimate that a *U. hadrourus*/*U. caudimaculatus* lineage extends back at least 1 million years, and possibly 2.5 million years ago to the Early Pleistocene (Watts & Baverstock, 1994; Bryant *et al.*, 2011). Currently no Early Pleistocene fossil sites are known from north-east Queensland, while in north-west Queensland, the Early Pleistocene Rackham's Roost fauna from Riversleigh, though rich in xeric-adapted rodents, understandably lacks *Uromys* (Godthelp, 1999). Therefore, the mesic-adapted habitats were probably already restricted to the wetter eastern seaboard by the Early Pleistocene. Thus, arrival, speciation, isolation, and extinction of species of *Uromys* in eastern Queensland potentially occurred all within the last two million years.

Based on current palaeoclimatic and palaeoenvironmental proxies across continental Australia (Christensen *et al.*, 2017) and more local Neogene records (Henderson & Nind, 2014), it is likely that corridors of mesic habitat were restricted to the eastern seaboard of Australia, including central-eastern and north-eastern Queensland, during the Quaternary. Therefore, connectivity of these mesic habitats would have been needed for ancestral *Uromys* to disperse southwards along the eastern seaboard to at least the Mount Etna region, subsequently producing *U. aplini*.

Local extinction of *U. aplini* occurred at Mount Etna sometime after 205–170 ka as the environment transitioned from closed wet rainforest to dry-adapted habitats (Hocknull *et al.*, 2007). Sometime after this, *U. caudimaculatus* arrived in the region for the first time, likely dispersing southward along a route similar to that taken by the ancestor of *U. aplini*. The age of the *U. caudimaculatus* lineage is considered to be > 1 Ma (Bryant *et al.*, 2011) but the species has not been detected in the > 500–280 ka deposits at Mount Etna. This dispersal may have occurred sometime after the extinction of *U. aplini* (c. 205–170 ka), during a period of mesic return. Therefore, corridors of habitat must have existed to allow the dispersal of this taxon south to the Mount Etna region. Until its local extinction, *Uromys caudimaculatus* existed in this region after 50 ka but prior to the onset of the Last Glacial Maximum. The exact timing of the local extinction of *U. caudimaculatus* remains unresolved. Additional dating of layers containing this taxon could potentially refine this local extinction timeline.

Together, these two records of *Uromys* demonstrate multiple southern dispersals and subsequent local extinctions during the Pleistocene, with the likelihood that these dispersals required the crossing of several biogeographical barriers identified (Bryant & Krosch, 2016) along the eastern seaboard in north-east and central-eastern Queensland (Fig. 1).

Combining the spatio-temporal record of *Uromys* along with our preliminary phylogenetic hypothesis suggests that the mesic regions of the Australian mainland supported the initial radiation of *Uromys* (*Uromys*), with a separate earlier lineage diversifying into the taxa contained within *Uromys* (*Cyromys*) that possibly occupied the emergent Solomon Islands. Subsequent dispersal of the Australian clade throughout New Guinea is contrary to what would be expected on the basis of the species richness of *Uromys* currently found today throughout the New Guinea to Solomon Islands region, compared to that of mainland Australia. It is, however, recognized that throughout much of the Cenozoic, bias of mesic faunal extinction resulted in an overall shift of mainland Australian biomes toward more xeric-adaptation, thus mesic biomes are now significantly under-represented (Byrne *et al.*, 2011). The timing of these extinctions, and the effect of these on our understanding of present-day biogeography and phylogeography remains poor, without further study of the fossil record. Establishing the fossil record of these mesic biome lineages is crucial to understanding the timing and tempo of these biogeographical changes. *Uromys* represents just one group that can provide data on the evolution of this significant biome.

Palaeoecology of *Uromys*

Living species of *Uromys* are semiarboreal omnivores (Breed & Ford, 2007). The ability to access food resources in the canopy (e.g., fruits, before they fall to the forest floor) has been suggested as a competitive advantage for species of *Uromys* (Rader & Krockenberger, 2006); this probably played a role in resource partitioning in the species-rich Mount Etna Middle Pleistocene rainforest. The larger size of most species (*U. hadrourus* and *U. porculus* being exceptions) allows them to utilize food resources that are inaccessible to smaller rodents. For example, large species of *Uromys* in north Queensland are known to gnaw through the hard, thick shells of coconuts (Watts & Aslin, 1981) and are also infamous for opening metal traps (Elliot traps) to steal bait or prey upon smaller mammals (Laurance *et al.*, 1993; Eric Vanderduys, pers. comm. January 2020). Furthermore, there is evidence that smaller murines actively avoid large species of *Uromys* (Leung, 2008) suggesting that an “ecology of fear” (Brown *et al.*, 1999) may have a role in structuring small mammal assemblages, at least on a local scale. *Uromys aplini* is the largest murine in the Mount Etna deposits, and may have behaved much like its extant relatives, robbing large seeds, consuming fruits and insects, and generally terrorizing the smaller vertebrates.

Extinction of *Uromys* in central Queensland

The majority of rainforest-inhabiting species at Mount Etna became extinct after 280 ka (minimum age of site QML1313). But a small number of rainforest-adapted species, e.g., *Dendrolagus* sp. (Hocknull *et al.*, 2007) and *Antechinus yuna* (Cramb & Hocknull, 2010) persisted for some tens of thousands of years, and appear in low numbers in QML1312, dated to 205–170 ka (Hocknull *et al.*, 2007). *Uromys aplini* is one of these, and is represented by a single specimen in QML1312. The possibility of this specimen being derived from faunal mixing (e.g., a time-averaged or reworked deposit) can be discounted as the assemblage of surviving rainforest taxa shows clear selection of certain

species. For example, multiple specimens of *Antechinus yuna* are present, yet *Antechinus yammal* is absent, despite these two species being ubiquitous in older rainforest assemblages (Cramb & Hocknull, 2010).

The late survival of *U. aplini* implies some degree of ecological flexibility, a reasonable proposition in light of the apparent ability of extant *U. caudimaculatus* to make use of a variety of habitats in north Queensland (Moore, 2008). Despite this adaptability, *U. aplini* disappeared from the local record prior to deposition of site QML1456 (<80 ka, Price *et al.*, 2015). *Uromys caudimaculatus* appears intermittently in the lower, older spits of QML1456, before apparently becoming locally extinct soon after 50 ka. The loss of both species may be explicable by an increasingly dry regional climate during the latter part of the Pleistocene and associated replacement of closed-canopy forests by open habitats. Despite a return to more mesic conditions during the Holocene, and deposits representing Holocene-aged accumulations, there is no evidence of *Uromys* returning to the Mount Etna area.

ACKNOWLEDGEMENTS. The authors wish to thank Kristen Spring and QM geosciences staff for curation of specimens, Heather Janetzki, Sandy Ingleby, Karen Roberts, Ken Aplin, and Fred Ford for access to comparative material, the Willi Hennig Society for providing phylogenetic software, Tyrone Lavery for providing an additional datum, Noel and Jeanette Sands and family for assistance in the field, all staff at Capricorn Caves including the Augusteyn family, for their support of palaeontological research, all researchers, honoraries, and volunteers involved in the Mount Etna project, and Liz Cramb for supporting her husband's palaeontology habit. Collection of material for this project was supported by the Ian Potter Foundation and ARC Linkage Grant (LP0453664).

References

- Alston, E. R. 1876. On the classification of the Order Glires. *Proceedings of the Zoological Society of London* 1876: 61–98.
<https://doi.org/10.1111/j.1096-3642.1876.tb02543.x>
- Aplin, K. P. 2006. Ten million years of rodent evolution in Australasia: phylogenetic evidence and a speculative historical biogeography. In *Evolution and Biogeography of Australasian Vertebrates*, ed. J. R. Merrick, M. Archer, G. M. Hickey, and M. S. Y. Lee, pp. 707–744. Oatlands, Sydney: Auscipub.
- Aplin, K. P., and T. F. Flannery. 2017. *Uromys anak*. *The IUCN Red List of Threatened Species* 2017: e.T22800A22447286.
<https://doi.org/10.2305/IUCN.UK.2017-2.RLTS.T22800A22447286.en>
- Aplin, K. P., and K. M. Helgen. 2010. Quaternary murid rodents of Timor part I: new material of *Coryphomys buehleri* Schaub, 1937, and description of a second species of the genus. *Bulletin of the American Museum of Natural History* 341: 1–80.
<https://doi.org/10.1206/692.1>
- Aplin, K. P., K. M. Helgen, and J. W. Winter. 2017. *Uromys caudimaculatus*. *The IUCN Red List of Threatened Species* 2017: e.T22801A22446882.
<https://doi.org/10.2305/IUCN.UK.2017-2.RLTS.T22801A22446882.en>
- Aplin, K. P., J. M. Pasveer, and W. E. Boles. 1999. Late Quaternary vertebrates from the Bird's Head Peninsula, Irian Jaya, Indonesia, including descriptions of two previously unknown marsupial species. *Records of the Western Australian Museum*, Supplement no. 57: 351–387.
- Breed, W. G., and K. P. Aplin. 1995. Sperm morphology of murid rodents from New Guinea and the Solomon Islands—phylogenetic implications. *Australian Journal of Zoology* 43: 17–30.
<https://doi.org/10.1071/ZO9950017>
- Breed, W. G., and F. Ford. 2007. *Native Mice and Rats*. Collingwood: CSIRO Publishing, 185 pp.
<https://doi.org/10.1071/9780643095595>
- Brown, J. S., J. W. Laundré, and M. Gurung. 1999. The ecology of fear: optimal foraging, game theory, and trophic interactions. *Journal of Mammalogy* 80: 385–399.
<https://doi.org/10.2307/1383287>
- Bryant, L. M., S. C. Donnellan, D. A. Hurwood, and S. J. Fuller. 2011. Phylogenetic relationships and divergence date estimates among Australo-Papuan mosaic-tailed rats from the *Uromys* division (Rodentia: Muridae). *Zoologica Scripta* 40: 433–447.
<https://doi.org/10.1111/j.1463-6409.2011.00482.x>
- Bryant, L. M., and M. N. Krosch. 2016. Lines in the land: a review of evidence for eastern Australia's major biogeographical barriers to closed forest taxa. *Biological Journal of the Linnean Society* 119: 238–264.
<https://doi.org/10.1111/bj.12821>
- Byrne, M., D. A. Steane, L. Joseph, D. K. Yeates, G. J. Jordan, D. Crayn, K. Aplin, D. J. Cantrill, L. G. Cook, M. D. Crisp, J. S. Keogh, J. Melville, C. Moritz, N. Porch, J. M. K. Sniderman, P. Sunnucks, and P. H. Weston. 2011. Decline of a biome: evolution, contraction, fragmentation, extinction and invasion of the Australian mesic zone biota. *Journal of Biogeography* 38: 1635–1656.
<https://doi.org/10.1111/j.1365-2699.2011.02535.x>
- Christensen, B. A., W. Renema, J. Henderiks, D. De Vleeschouwer, J. Groeneveld, I. S. Castañeda, L. Reuning, K. Bogus, G. Auer, T. Ishiwa, and C. M. McHugh. 2017. Indonesian throughflow drove Australian climate from humid Pliocene to arid Pleistocene. *Geophysical Research Letters* 44: 6914–6925.
<https://doi.org/10.1002/2017GL072977>
- Cramb, J., S. Hocknull, and G. E. Webb. 2009. High diversity Pleistocene rainforest dasyurid assemblages with implications for the radiation of the Dasyuridae. *Austral Ecology* 34: 663–669.
<https://doi.org/10.1111/j.1442-9993.2009.01972.x>
- Cramb, J., and S. Hocknull. 2010. Two new species of *Antechinus* Macleay (Dasyuridae: Marsupialia) from mid-Pleistocene cave deposits in eastern central Queensland. *Australian Mammalogy* 32: 127–144.
<https://doi.org/10.1071/AM09025>
- Flannery, T. F. 1995a. *Mammals of New Guinea*. Chatswood: Reed Books, 568 pp.
- Flannery, T. F. 1995b. *Mammals of the South-west Pacific and Moluccan Islands*. Chatswood: Reed Books, 464 pp.
- Godthelp, H. 1999. The Australian rodent fauna, flotsam, or just fleet footed? In *Where Worlds Collide: Faunal and Floral Migrations and Evolution in SE Asia-Australasia*, ed. I. Metcalfe, J. M. B. Smith, M. Morwood, and I. Davidson, pp. 319–321. Armidale: University of New England.
- Gray, J. E. 1867. Notes on the variegated or yellow-tailed rats of Australasia. *Proceedings of the Zoological Society of London* 1867: 597–600.
- Groves, C. P., and T. F. Flannery. 1994. A revision of the genus *Uromys* Peters, 1867 (Muridae: Mammalia) with descriptions of two new species. *Records of the Australian Museum* 46(2): 145–169.
<https://doi.org/10.3853/j.0067-1975.46.1994.12>
- Hammer, Ø., D. A. T. Harper, and P. D. Ryan. 2001. PAST: paleontological statistics software package for education and data analysis. *Palaeontologia Electronica* 4(1), 9 pp.
- Hand, S. J. 1984. Australia's oldest rodents: master mariners from Malaysia. In *Vertebrate Zoogeography and Evolution in Australia*, ed. M. Archer and G. Clayton, pp. 905–912. Carlisle: Hesperia Press.

- Henderson, R. A., and M. A. P. Nind. 2014. Pliocene aridity and Neogene landscape evolution recorded by a fluvial sediment system (Campaspe Formation) in northeast Queensland. *Australian Journal of Earth Sciences* 61: 1041–1059. <https://doi.org/10.1080/08120099.2014.965745>
- Hocknull, S. A. 2005. Ecological succession during the late Cainozoic of central eastern Queensland: extinction of a diverse rainforest community. *Memoirs of the Queensland Museum* 51(1): 39–122.
- Hocknull, S. 2009. *Late Cainozoic Rainforest Vertebrates from Australopapua: Evolution, Biogeography and Extinction*. Unpublished Ph.D. thesis. University of New South Wales, Sydney, 627 pp.
- Hocknull, S. A., J.-x. Zhao, Y.-x. Feng, and G. E. Webb. 2007. Responses of Quaternary rainforest vertebrates to climate change in Australia. *Earth and Planetary Science Letters* 264: 317–331. <https://doi.org/10.1016/j.epsl.2007.10.004>
- Illiger, C. 1811. *Prodromus systematis mammalium et avium additis terminis zoographicis utriusque classis, eorumque versione germanica*. Berlin: C. Salfeld, 330 pp. <https://doi.org/10.5962/bhl.title.106965>
- Jackson, S., and C. Groves. 2015. *Taxonomy of Australian Mammals*. Clayton South: CSIRO Publishing, 536 pp. <https://doi.org/10.1071/9781486300136>
- Kennerley, R. 2016. *Uromys siebersi* (errata version published in 2017). *The IUCN Red List of Threatened Species* 2016: e.T136493A115209020. <https://doi.org/10.2305/IUCN.UK.2016-3.RLTS.T136493A22446733.en>
- Kreffit, G. 1867. Notes on the mammals and birds of Cape York: with description of two new rodents of the genus *Hapalotis*. *Proceedings of the Zoological Society of London* 1867: 316–319
- Laurance, W. F., J. Garesche, and C. W. Payne. 1993. Avian nest predation in modified and natural habitats in tropical Queensland: an experimental study. *Wildlife Research* 20: 711–723. <https://doi.org/10.1071/WR9930711>
- Lavery, T. H. 2019. *Uromys vika*. *The IUCN Red List of Threatened Species* 2019: e.T120569706A120569709. <https://doi.org/10.2305/IUCN.UK.2019-1.RLTS.T120569706A120569709.en>
- Lavery, T. H., and H. Judge. 2017. A new species of giant rat (Muridae, *Uromys*) from Vangunu, Solomon Islands. *Journal of Mammalogy* 98: 1518–1530. <https://doi.org/10.1093/jmammal/gyx116>
- Lazzari, V., J.-P. Aguilar, and J. Michaux. 2010. Intraspecific variation and micro-macroevolution connection: illustration with the late Miocene genus *Progonomys* (Rodentia, Muridae). *Paleobiology* 36: 641–657. <https://doi.org/10.1666/09046.1>
- Lecompte, E., K. Aplin, C. Denys, F. Catzeflis, M. Chades, and P. Chevret. 2008. Phylogeny and biogeography of African Murinae based on mitochondrial and nuclear gene sequences, with a new tribal classification of the subfamily. *BMC Evolutionary Biology* 8: 199. <https://doi.org/10.1186/1471-2148-8-199>
- Leung, L. K. P. 2008. Cape York Melomys *Melomys capensis* Tate, 1951. In *Mammals of Australia*, 3rd edition, ed. S. M. Van Dyck and R. Strahan, pp. 669–671. Sydney: Reed New Holland.
- Lidicker Jr, W. Z., and P. V. Brylski. 1987. The conilurine rodent radiation of Australia, analyzed on the basis of phallic morphology. *Journal of Mammalogy* 68: 617–641. <https://doi.org/10.2307/1381596>
- Maddison, W. P., and D. R. Maddison. 2019. Mesquite: a modular system for evolutionary analysis. Version 3.61 <http://www.mesquiteproject.org/>
- Moore, L. A. 2008. Giant White-tailed Rat *Uromys caudimaculatus* (Kreffit, 1867). In *Mammals of Australia*, 3rd edition, ed. S. M. Van Dyck and R. Strahan, pp. 675–677. Sydney: Reed New Holland.
- Moore, L. A., and J. W. Winter. 2008. Pygmy White-tailed Rat *Uromys hadrourus* (Winter, 1984). In *Mammals of Australia*, 3rd edition, ed. S. M. Van Dyck and R. Strahan, pp. 677–679. Sydney: Reed New Holland.
- Musser, G. G. 1981. The giant rat of Flores and its relatives east of Borneo and Bali. *Bulletin of the American Museum of Natural History* 169: 67–175.
- Musser, G. G., and M. D. Carleton. 2005. Superfamily Muroidea. In *Mammal Species of the World: A Taxonomic and Geographic Reference* volume 2, 3rd edition, ed. D. E. Wilson and D. M. Reeder, pp. 894–1531. Baltimore: The Johns Hopkins University Press.
- O'Connor, S., K. P. Aplin, M. Spriggs, P. Veth, and L. K. Ayliffe. 2002. From savannah to rainforest: changing environments and human occupation at Liang Lembudu, Aru Islands, Maluku (Indonesia). In *Bridging Wallace's Line: The Environmental and Cultural History and Dynamics of the Southeast Asian-Australian Region*, ed. P. Kershaw, B. David, N. Tapper, D. Penny, and J. Brown, pp. 279–306. Advances in Geocology Series, no. 34. Reiskirchen: Catena Verlag.
- Peters, W. 1867. Über eine neue Gattung von Nagern, *Uromys*, aus Nordaustralien. *Monatsberichte der Königlich Preussischen Akademie des Wissenschaften zu Berlin* 1867: 343–345.
- Piper, K. J., E. M. G. Fitzgerald, and T. H. Rich. 2006. Mesozoic to early Quaternary mammal faunas of Victoria, south-east Australia. *Palaeontology* 49: 1237–1262. <https://doi.org/10.1111/j.1475-4983.2006.00595.x>
- Price, G. J. 2012. Plio-Pleistocene climate and faunal change in central eastern Australia. *Episodes* 35: 160–165. <https://doi.org/10.18814/epiiugs/2012/v35i1/015>
- Price, G. J., and S. A. Hocknull. 2011. *Invictokoala monticola* gen. et sp. nov. (Phascolarctidae, Marsupialia), a Pleistocene plesiomorphic koala holdover from Oligocene ancestors. *Journal of Systematic Palaeontology* 9(2): 327–335. <https://doi.org/10.1080/14772019.2010.504079>
- Price, G. J., J. Louys, J. Cramb, Y.-x. Feng, J.-x. Zhao, S. A. Hocknull, G. E. Webb, A. D. Nguyen, and R. Joannes-Boyau. 2015. Temporal overlap of humans and giant lizards (Varanidae; Squamata) in Pleistocene Australia. *Quaternary Science Reviews* 125: 98–105. <https://doi.org/10.1016/j.quascirev.2015.08.013>
- Rader, R., and A. Krockenberger. 2006. Does resource availability govern vertical stratification of small mammals in an Australian lowland tropical rainforest? *Wildlife Research* 33: 571–576. <https://doi.org/10.1071/WR04108>
- Robins, J. H., P. A. McLenachan, M. J. Phillips, B. J. McComish, E. Matisoo-Smith, and H. A. Ross. 2010. Evolutionary relationships and divergence times among the native rats of Australia. *BMC Evolutionary Biology* 10: 375. <https://doi.org/10.1186/1471-2148-10-375>
- Rowe, K. C., M. L. Reno, D. M. Richmond, R. M. Adkins, and S. J. Steppan. 2008. Pliocene colonization and adaptive radiations in Australia and New Guinea (Sahul): multilocus systematics of the old endemic rodents (Muroidea: Murinae). *Molecular Phylogenetics and Evolution* 47: 84–101. <https://doi.org/10.1016/j.ympev.2008.01.001>
- Steppan, S. J., and J. J. Schenk. 2017. Muroid rodent phylogenetics: 900-species tree reveals increasing diversification rates. *PLoS ONE* 12(8): e0183070. <https://doi.org/10.1371/journal.pone.0183070>
- Swofford, D. L. 2001. Paup*: phylogenetic analysis using parsimony (and other methods) 4.0. B5.
- Tate, G. H. H. 1951. Results of the Archbold Expeditions. No. 65. The rodents of Australia and New Guinea. *Bulletin of the American Museum of Natural History* 97: 189–423.
- Tate, G. H. H., and R. Archbold. 1935. Results of the Archbold Expeditions. No. 3. Twelve apparently new forms of Muridae (other than *Rattus*) from the Indo-Australian region. *American Museum Novitates* 803(9): 1–9.

- Thomas, O. 1888. Diagnoses of six new mammals from the Solomon Islands. *Annals and Magazine of Natural History* (6)1: 155–158.
<https://doi.org/10.1080/00222938809460693>
- Thomas, O. 1904. On some mammals from British New Guinea presented to the National Museum by Mr. C. A. W. Monckton, with descriptions of other species from the same region. *Annals and Magazine of Natural History* (7)14: 397–403.
<https://doi.org/10.1080/03745480409443026>
- Thomas, O. 1907. On three new mammals from British New Guinea. *Annals and Magazine of Natural History* (7)20: 70–74.
<https://doi.org/10.1080/00222930709487303>
- Thomas, O. 1910. New genera of Australasian Muridae. *Annals and Magazine of Natural History* (8)6: 506–508.
<https://doi.org/10.1080/00222931008692883>
- Thomas, O. 1923a. The Godman Exploration Fund: list of mammals from North Queensland collected by Mr. T. V. Sherrin. *Annals and Magazine of Natural History* (9)11: 170–178.
<https://doi.org/10.1080/00222932308632835>
- Thomas, O. 1923b. A new *Uromys* from the Kei Islands. *Treubia* 3: 422.
- Upham, N. S., J. A. Esselstyn, and W. Jetz. 2019. Inferring the mammal tree: species-level sets of phylogenies for questions in ecology, evolution, and conservation. *PLOS Biology* 17(12): e3000494.
<https://doi.org/10.1371/journal.pbio.3000494>
- Watts, C. H. S., and H. J. Aslin. 1981. *The Rodents of Australia*. Sydney: Angus & Robertson.
- Watts, C. H. S., and P. R. Baverstock. 1994. Evolution in New Guinean Muridae (Rodentia) assessed by microcomplement fixation of albumin. *Australian Journal of Zoology* 42: 295–306.
<https://doi.org/10.1071/ZO9940295>
- Winter, J. W. 1983. Thornton Peak *Melomys*. In *The Complete Book of Australian Mammals*, ed. R. Strahan, p. 379. Sydney: Angus & Robertson.
- Winter, J. W. 1984. The Thornton Peak *Melomys*, *Melomys hadrourus* (Rodentia: Muridae): a new rainforest species from northeastern Queensland, Australia. *Memoirs of the Queensland Museum* 21: 519–539.
- Woinarski, J., and A. A. Burbidge. 2016. *Uromys hadrourus*. *The IUCN Red List of Threatened Species* 2016: e.T22802A22446971.
<https://doi.org/10.2305/IUCN.UK.2016-1.RLTS.T22802A22446971.en>

Appendix 1. List of modern specimens examined.

Uromys anak: AM M.15633, AM M.15634, AM M.15645, AM M.15646, AM M.15647, AM M.15753, AM M.15754, AM M.15854, AM M.16695, AM M.32337, AM M.38676, AM M.38702, AM M.38864, QMJM3838.

Uromys caudimaculatus: CM705, QMJ2344, QMJ5907, QMJ5908, QMJ6349, QMJ9304, QMJ9386, QMJ9387, QMJ9388, QMJ9389, QMJ9390, QMJ9454, QMJ9455, QMJ10131, QMJ10133, QMJ10134, QMJ11512, QMJ16181, QMJ16187, QMJ16450, QMJ16725, QMJ16768, QMJ16772, QMJM17309, QMJ17609, QMJ17610, QMJ17611, QMJ20347, QMJ22127, QMJ22538, QMJ22540, QMJ22606, QMJ22607, QMJ23023, QMJM1001, QMJM8738, QMJM10038, QMJM18470, QMJM21138.

Uromys hadrourus: QMJM504, QMJM2173, QMJM8146.

Uromys neobritannicus: AM M.20689, NMVC6890.

Uromys rex: AM M.13594.

Uromys sherrini: CM10822, QMJ5907, QMJ5908, QMJ8000, QMJ16725, QMJ17612, QMJ17613, QMJ17614, QMJ21272, QMJ22539, QMJ22606.
